STATISTICAL RELATIONSHIP BETWEEN THE NORTH ATLANTIC OSCILLATION AND THE CLIMATE OF TURKEY

by

Mustafa Tufan Turp

B.S., Physics, Yıldız Technical University, 2006

Submitted to the Institute for Graduate Studies in
Science and Engineering in partial fulfillment of
the requirements for the degree of
Master of Science

Graduate Program in Computational Science and Engineering

Boğaziçi University

2010

ACKNOWLEDGMENTS

I would like to express my gratitude to my thesis advisor, Prof. M. Levent Kurnaz, for his invaluable guidance, support, motivation and endless patience during my MS thesis.

I would like to thank Şükrü Murat Cebeci, Şükriye Öz and Zerrin Demirörs for helping me to provide necessary data used in this study.

It is a pleasure for me to thank my friends Cihat Kurt, Hamza Altınsoy, Alperen Yüncü, Seda Özaskan and Gizem Çalık for their unforgettable efforts in every steps of this research. They made the sleepless nights more enjoyable together.

I would also like to thank Tuğba Öztürk, Sena Pekkendir, Rümeysa Muş, Pelin Çeber, Merve Aslı, Büşra İnce, Berna Dündar, Canan Şahin and all members of "iklimBU" for giving me their everlasting friendships and joyful helps.

Finally, the biggest thanks are to my mother Perihan Turp, father Halil Şit Turp, elder sisters Deniz Turp and Derya Turp for their everlasting encouragement and support that they have shown to me. They make my life lovable. This thesis is dedicated to them.

ABSTRACT

STATISTICAL RELATIONSHIP BETWEEN THE NORTH ATLANTIC OSCILLATION AND THE CLIMATE OF TURKEY

Over the middle and high latitudes of the Northern Hemisphere, roughly a dozen distinct teleconnection patterns can be identified. One of the most prominent is the North Atlantic Oscillation, which refers to changes in the atmospheric sea level pressure difference between the Arctic and the subtropical Atlantic. Although it is the only teleconnection pattern evident throughout the year in the Northern Hemisphere, the climate anomalies associated with the North Atlantic Oscillation are largest during the boreal winter months when the atmosphere is dynamically the most active. If we can predict the changes occur on the North Atlantic Oscillation, we can also make better predictions about the climate change observed in our country. In this thesis, the station data of temperature and precipitation belong to 1980-2000, the station based and calculated NAO indices, and the results derived from RegCM (Regional Climate Model) for the same period were used to reveal the effects of the North Atlantic Oscillation on Turkey's temperature and precipitation regime. The statistical relationship between the NAO and the temperature and precipitation variables of Turkey was also investigated.

ÖZET

KUZEY ATLANTİK SALINIMI İLE TÜRKİYE'NİN İKLİMİ ARASINDAKİ İSTATİSTİKSEL İLİŞKİ

Kuzey Yarımkürenin orta ve yüksek enlemleri üzerinde yaklaşık bir düzine farklı iklim deseni tanımlanmaktadır. Bunlardan en etkin olanı ise Kuzey Atlantik Salınımı'dır. Kuzey Atlantik Salınımı (NAO), Arktik ve dönencealtı bölgeler arasında görülen deniz seviyesindeki atmosferik basınç değişimleri olarak tanımlanır. Her ne kadar Kuzey Atlantik Salınımı, Kuzey Yarımküre'de yıl boyunca gözlemlenen tek iklim deseni olsa da Kuzey Atlantik Salınımı ile ilişkili iklimsel sapmalar atmosferin dinamik olarak en aktif olduğu boreal kış aylarında daha büyüktür. NAO'daki değişimleri önceden tahmin edebilmek bir anlamda ülkemizdeki iklim değişikliğinin tahminine de yardımcı olacaktır. Bu çalışmada Türkiye'de 1980–2000 yılları arasında ölçülen sıcaklık ve yağış değerleri ve bölgesel iklim modellemesi RegCM'den elde edilen sonuçlar ile aynı tarihler arasında hesaplanan ve ölçülen NAO endeksleri arasındaki korelasyonlar incelenerek Avrupa, Akdeniz ve Avrasya üzerinde de etkisini gösteren NAO'nun Türkiye'nin sıcaklık ve yağış rejimleri ile olan istatistiksel ilişkisi araştırılmıştır

TABLE OF CONTENTS

LIST OF FIGURES

LIST OF TABLES

LIST OF SYMBOLS / ABBREVIATIONS

a	y-intercept of the regression equation
b	Slope of the line in the regression equation
$\varepsilon(X)$	Expected value of X
$\varepsilon(Y)$	Expected value of Y
σ_X	Correlation coefficient of X
σ_Y	Correlation coefficient of Y
CRU	Climatic Research Unit of East Anglia University
DJFM	December-January-February-March
EA	East Atlantic pattern
EATL/WRUS	East Atlantic/Western Russia pattern
ENSO	El Nino/Southern Oscillation
EOF	Empirical Orthogonal Functions
EP-NP	East Pacific-North Pacific pattern
GCM	Global Climate Model
ICBC	Initial Conditions and Boundary Conditions
NAO	North Atlantic Oscillation
NAOI	North Atlantic Oscillation Indices
NH	Northern Hemisphere
NOAA	National Oceanic and Atmospheric Administration
PNA	Pacific/North American pattern
PT	Pacific Transition pattern

RCM	Regional Climate Model
SCAND	Scandinavia pattern
SLP	Sea Level Pressure
SST	Sea Surface Temperature
TNH	Tropical/Northern Hemisphere pattern
UCAR	University Corporation for Atmospheric Research
Var	Variance
WP	West Pacific pattern

1. INTRODUCTION

1.1. Northern Hemisphere Teleconnection Patterns

The atmospheric circulation is well-known to exhibit substantial variability. This variability reflects weather patterns and circulation systems that occur on many time scales, lasting from a few days, to a few weeks, to a few months, to several years, to several centuries.

Simultaneous variations in weather and climate over widely separated points on earth have long been noted in the meteorological literature. Such variations are known as "teleconnections" or "teleconnection patterns". The term "teleconnection pattern" refers to a recurring and persistent, large-scale pattern of pressure and circulation anomalies that span vast geographical areas. Teleconnection patterns are also referred to as preferred modes of low-frequency or long time scale variability. Although these patterns typically last for several weeks to several months, they can sometimes be prominent for several consecutive years, thus reflecting an important part of both the interannual and interdecadal variability of the atmospheric circulation. Many of the teleconnection patterns are also planetary-scale in nature, and span entire ocean basins and continents. For example, some patterns span the entire North Pacific basin, while others extend from eastern North America to central Europe. Still others cover nearly all of Eurasia. In the extratropics, teleconnections link neighboring regions mainly through the transient behavior of atmospheric planetary-scale waves. Consequently, some regions may be cooler than average, while thousands of kilometers away warmer conditions prevail. Though the precise nature and shape of these structures vary to some extent according to the statistical methodology and the data set employed in the analysis, consistent regional characteristics that identify the most conspicuous patterns emerge [1, 2].

All teleconnection patterns are a naturally occurring aspect of our chaotic atmospheric system and they can arise primarily as a reflection of internal atmospheric dynamics. They reflect large-scale changes in the atmospheric wave and jet stream patterns,

and influence temperature, rainfall, storm tracks, and jet stream location or intensity over vast areas [1, 3].

Hence, they are often the culprit responsible for abnormal weather patterns occurring simultaneously over seemingly vast distances. In the Northern Hemisphere extratropics, ten prominent teleconnection patterns can be identified throughout the year. We can split these patterns into three regions with respect to their affected regions: prominent patterns over the North Pacific or North America, prominent patterns over Eurasia and prominent patterns over the North Atlantic. Each one of all these patterns is represented by multiple indices in two different phases (positive and negative) and every phase has various influences on the effected places [1, 3].

1.1.1. Prominent Patterns over the North Pacific/North America

Over the North Pacific region, there are five prominent patterns which have different time-scales: West Pacific pattern (WP), East Pacific-North Pacific pattern (EP-NP), Pacific/North American pattern (PNA), Tropical/Northern Hemisphere pattern (TNH) and Pacific Transition pattern (PT).

1.1.1.1. West Pacific Pattern. The West Pacific Pattern is a primary mode of low-frequency variability over the North Pacific and it exists in all months. During winter and spring, the pattern consists of a north-south dipole of anomalies, with one center located over the Kamchatka Peninsula and another broad center of opposite sign covering portions of southeastern Asia and the western subtropical North Pacific. Therefore, strong positive or negative phases of this pattern reflect pronounced zonal and meridional variations in the location and intensity of the entrance region of the Pacific or East Asian jet steam. These anomalies exhibit a strong northward shift from winter to summer, which is consistent with the observed northward shift of the East Asian jet stream. A third anomaly center is located over the eastern North Pacific and southwestern United States in all seasons [1, 3, 4].

The positive phase of the WP pattern is associated with above-average temperatures over the lower latitudes of the western North Pacific in both winter and spring and with below-average temperatures over eastern Siberia in all seasons. It is also associated with

above-average precipitation in all seasons over the high latitudes of the North Pacific, and below-average precipitation across the central North Pacific especially during the winter and spring [1, 3].

1.1.1.2. East Pacific – North Pacific Pattern. The East Pacific – North Pacific Pattern is a spring-summer-fall pattern with three main anomaly centers. The positive phase of this pattern features positive height anomalies located over Alaska/ Western Canada, and negative anomalies over the central North Pacific and eastern North America. Strong positive phases of the EP-NP pattern are associated with a southward shift and intensification of the Pacific jet stream from eastern Asia to the eastern North Pacific, followed downstream by an enhanced anticyclonic circulation over western North America, and by an enhanced cyclonic circulation over the eastern United States. Strong negative phases of the pattern are associated with circulation anomalies of opposite sign in these regions [1, 3, 4].

The positive phase of the EP-NP pattern is associated with above-average surface temperatures over the eastern North Pacific and below-average temperatures over the central North Pacific and eastern North America. The main precipitation anomalies associated with this pattern reflect above-average precipitation in the area north of Hawaii and below-average precipitation over southwestern Canada [1, 3, 4].

1.1.1.3. Pacific – North American Pattern. The Pacific – North American Pattern is one of the most prominent modes of low-frequency variability in the Northern Hemisphere extratropics. The PNA pattern is also strongly influenced by the El Nino/Southern Oscillation (ENSO) phenomenon, although it is a natural internal mode of climate variability. PNA pattern's positive phase tends to be associated with Pacific warm episodes (El Nino) and the negative phase of it tends to be associated with Pacific cold episodes (La Nina). The positive phase of the PNA pattern features above-average heights in the vicinity of Hawaii and over the intermountain region of North America, and below-average heights located south of the Aleutian Islands and over the southeastern United States. The PNA pattern is associated with strong fluctuations in the strength and location of the East Asian jet stream. The positive phase is associated with an enhanced East Asian jet stream and with an eastward shift in the jet exit region toward the western United States. The negative phase is associated with a westward retraction of that jet stream toward eastern Asia,

blocking activity over the high latitudes of the North pacific, and a strong split-flow configuration over the central North Pacific [1, 3, 4].

The positive phase of the PNA pattern is associated with above-average temperatures over western Canada and the extreme western United States, and below-average temperatures across the south-central and southeastern United States. The PNA tends to have little impact on surface temperature variability over North America during summer. The associated precipitation anomalies include above-average totals in the Gulf of Alaska extending into the Pacific Northwestern United States, and below-average totals over the upper Midwestern United States [1, 3, 4].

1.1.1.4. Tropical – Northern Hemisphere Pattern. The Tropical – Northern Hemisphere Pattern appears as a prominent wintertime mode during December-February. The positive phase of the TNH pattern features above-average heights over the Gulf of Alaska and from the Gulf of Mexico northeastward across the western North Atlantic, and below-average heights throughout eastern Canada [1, 3].

The TNH pattern reflects large-scale changes in both the location and eastward extent of the Pacific jet stream, and also in the strength and position of the climatological mean Hudson Bay Low. Thus, the pattern significantly modulates the flow of marine air into North America, as well as the southward transport of cold Canadian air into the north-central United States [1, 3].

The positive phase of the TNH pattern is associated with below-average surface temperatures throughout the western and central United States, and across central and eastern Canada. It is also associated with above-average precipitation across the central and eastern subtropical North Pacific, and below-average precipitation in the western United States and across Cuba, the Bahamas, and much of the central North Atlantic Ocean [1, 3].

1.1.1.5. Pacific Transition Pattern. The Pacific Transition Pattern is a leading mode which exists during August-September. This pattern captures anomalous wave-train of 500-hPa heights extending from the central subtropical North Pacific to the eastern United States. The positive phase of the PT pattern features above-average heights west of Hawaii and

across western North America, and below-average heights in the Gulf of Alaska and over the southeastern United States [1, 3].

The PT pattern is associated with above-average surface temperatures in the western subtropical North Pacific, the subtropical North Atlantic, and throughout western North America, and with below-average temperatures over the eastern half of the United States. The main precipitation departures associated with the PT pattern include above-average precipitation in the southeastern United States, and below-average precipitation near Hawaii and across the northern tier of the United States [1, 3].

1.1.2. Prominent Patterns over Eurasia

There are three prominent patterns over Eurasia that exist in all months: East Atlantic/Western Russia pattern (EATL/WRUS), Scandinavia pattern (SCAND) and Polar/Eurasia pattern.

1.1.2.1. East Atlantic/Western Russia Pattern. The East Atlantic/Western Russia pattern is one of three prominent teleconnection patterns and it affects Eurasia throughout year. The EATL/WRUS pattern consists of four main anomaly centers. The positive phase is associated with positive height anomalies located over Europe and northern China, and negative height anomalies located over the central North Atlantic and north of the Caspian Sea [1, 3].

The main surface temperature anomalies associated with the positive phase of the EATL/ WRUS pattern reflect above-average temperatures over eastern Asia, and below-average temperatures over large portions of western Russia and northeastern Africa. The main precipitation departures reflect generally above-average precipitation in eastern China and below-average precipitation across central Europe [1, 3].

1.1.2.2. Scandinavia Pattern. The Scandinavia pattern consists of a primary circulation center over Scandinavia, with weaker centers of opposite sign over western Europe and eastern Russia/ western Mongolia. The positive phase of this pattern is associated with positive height anomalies, sometimes reflecting major blocking anticyclones, over

Scandinavia and western Russia, while the negative phase of the pattern is associated with negative height anomalies in these regions [1, 3].

The positive phase of the SCAND is associated with below-average temperatures across central Russia and also over western Europe. It is also associated with above-average precipitation across central and southern Europe, and below-average precipitation across Scandinavia [1, 3].

1.1.2.3. Polar/Eurasia Pattern. The Polar/Eurasia pattern exists in all seasons. The positive phase of this pattern consists of negative height anomalies over the polar region, and positive anomalies over northern China and Mongolia. This pattern is associated with fluctuations in the strength of the circumpolar circulation, with the positive phase reflecting an enhanced circumpolar vortex and the negative phase reflecting a weaker than average polar vortex [1, 3, 4].

The Polar/Eurasian pattern is mainly associated with above-average temperatures in eastern Siberia and below-average temperatures in eastern China. It is also associated with above-average precipitation in the polar region north of Scandinavia [1, 3, 4].

The Polar/Eurasian pattern can exhibit strong low-frequency variability. For instance, a negative phase of the pattern prevailed during 1955-1961, followed by appositive phase during 1964/65-1969/70. Similar persistent negative and positive phases of the pattern were observed during the 1980s-1990s [1, 3, 4].

1.1.3. Prominent Patterns over the North Atlantic

Two prominent patterns appear over the North Atlantic region throughout the year: East Atlantic pattern (EA) and North Atlantic Oscillation (NAO).

1.1.3.1. East Atlantic Pattern. The East Atlantic pattern is a prominent mode of low-frequency variability over the North Atlantic and appears as a leading mode in all months. The EA pattern is structurally similar to the North Atlantic Oscillation, and consists of a

north-south dipole of anomaly centers spanning the North Atlantic from east to west [1, 3, 4].

The positive phase of the EA pattern is associated with above-average surface temperatures in Europe in all months and with below-average temperatures over the southern United States during January-May and in the north-central United States during July-October. It is also associated with above-average precipitation over northern Europe and Scandinavia, and with below-average precipitation across southern Europe [1, 3, 4].

The EA pattern exhibits very strong multi-decadal variability in the 1950-2004 record, with the negative phase prevailing during much of 1950-1976, and the positive phase occurring during much of 1977-2004. The positive phase of the EA pattern was particularly strong and persistent during 1997-2004, when 3-month running mean values routinely averaged 1.0-2.0 standard deviations above normal [1, 3, 4].

1.1.3.2. North Atlantic Oscillation. The North Atlantic Oscillation is one of the most prominent teleconnection patterns in all seasons even though it has been originally identified for the winter season. The NAO consists of a north-south dipole of anomalies with one center located over Greenland and the other center of opposite sign spanning the central latitudes of the North Atlantic between 35°N and 40°N. The positive phase of the NAO reflects below-normal heights and pressure across the high latitudes of the North Atlantic and above-normal heights and pressure over the central North Atlantic, the eastern United States and western Europe. The negative phase reflects an opposite pattern of height and pressure anomalies over these regions. Both phases of the NAO are associated with basin-wide changes in the intensity and location of the North Atlantic jet stream and storm track, and in large-scale modulations of the normal patterns of zonal and meridional heat and moisture transport. For this reason, these changes result in changes in temperature and precipitation patterns often extending from eastern North America to western and central Europe [1] – [6].

Strong positive phases of the NAO tend to be associated with above-average temperatures in the eastern United States and across northern Europe and below-average temperatures in Greenland and mostly across southern Europe and the Middle East. They

are also associated with above-average precipitation over northern Europe and Scandinavia in winter, and below-average precipitation over southern and central Europe. Opposite patterns of temperature and precipitation anomalies are typically observed during strong negative phases of the NAO. During particularly prolonged periods dominated by one particular phase of the NAO, anomalous height and temperature patterns are also often seen extending well into central Russia and north-central Siberia. The NAO exhibits considerable interseasonal and interannual variability, and prolonged periods of both positive and negative phases of the pattern are widely-used. The effects of the NAO have been examined in details on the next part [1] – [6].

2. STATISTICAL RELATIONSHIP BETWEEN THE NORTH ATLANTIC OSCILLATION INDEX AND THE TEMPERATURE AND PRECIPITATION REGIME OF TURKEY

2.1. The North Atlantic Oscillation Index

As has been mentioned before, various indices are in use to identify the northern hemisphere teleconnection patterns. In this context, the North Atlantic Oscillation pattern is also represented by the North Atlantic Oscillation indices (NAOI). There is not only one way to define the NAO, hence there are different index types depending on the calculation methods. For example, one basic approach is through conceptually simple-point correlation maps, identifying the NAO by regions of maximum negative correlation over the North Atlantic. The other technique is empirical orthogonal functions (EOF) analysis. EOF analysis is also known as principal component analysis. In this approach, the NAO is identified from the eigenvectors of the cross-covariance matrix, computed from the time variations of the grid point values of sea level pressure (SLP) or some other climate variable. The eigenvectors, each constrained to be spatially and temporally orthogonal to the others, are then scaled according to the amount of total data variance they explain. This linear approach assumes preferred atmospheric circulation states come in pairs, in which anomalies of opposite polarity have the same spatial structure. In contrast, climate anomalies can also be identified by cluster analysis techniques, which search for recurrent patterns of a specific amplitude and sign. Clustering algorithms identify weather or climate regimes, which correspond to peaks in the probability density function of the climate phase space [1, 7, 8].

In addition to these complex definitions, the easiest way is to use the station based index. The NAO is basically a climatic phenomenon, which occurs in the North Atlantic Ocean of fluctuations in the difference of atmospheric pressure at sea level between the Icelandic low and the Azores high. Most modern NAO indices can be derived from the numerical methods like as mentioned above, but the easiest one is derived from the simple difference in surface pressure anomalies between various northern and southern locations. There are three station based indices due to situations of the stations. First kind of index is

calculated by surface pressure difference between the stations Stykkisholmur in Reykjavik, Iceland and Lisbon, Portugal [2, 8, 9].

The second index type is calculated by surface pressure difference between the stations which situated in Ponta Delgada, Azores and Stykkisholmur, Iceland. Another index value is derived from surface pressure difference between Gibraltar station and Stykkisholmur station. As is seen, all of these definitions have in common the same northern point in Iceland and various southern points because of Stykkisholmur station is the only station in that region with a long record. A disadvantage of station-based indices is that they are fixed in space. Given the movement of the NAO centers of action through the annual cycle, such indices can only adequately capture NAO variability for parts of the year. Moreover, individual station pressures are significantly affected by small-scale and transient meteorological phenomena not related to the NAO, so contain noise [2, 8, 9].

2.1.1. Phases of the North Atlantic Oscillation Index

As is known, the North Atlantic Oscillation indices based on pressure measured at 2 stations. Stykkisholmur in Iceland is invariably used as the northern station, whereas either Ponta Delgada in Azores, Lisbon in Portugal and Gibraltar are used as the southern station. More recently studies have used Lisbon and Gibraltar even though many previous studies have used Ponta Delgada. The choice of southern station can make some differences. These differences especially occur in seasons other than winter. Nevertheless, these all the NAOI are defined by the similar numbers. For instance, Figure 2.1. shows the time series of the NAOI of the boreal winter (December-March) derived from the difference in sea level pressure between Lisbon in Portugal and Stykkisholmur, Reykjavik in Iceland from 1864 through 2007. As is shown in Figure 2.1. the indices of the NAO are identified in 2 different phases in consideration of the values of the indices. The positive values of the indices are named as “positive phase”, and the negative values of the indices are called as “negative phase”. Every phase of the Northern Oscillation indices produces unequal and various impacts (Figure 2.2.) [2, 10, 11, 12].

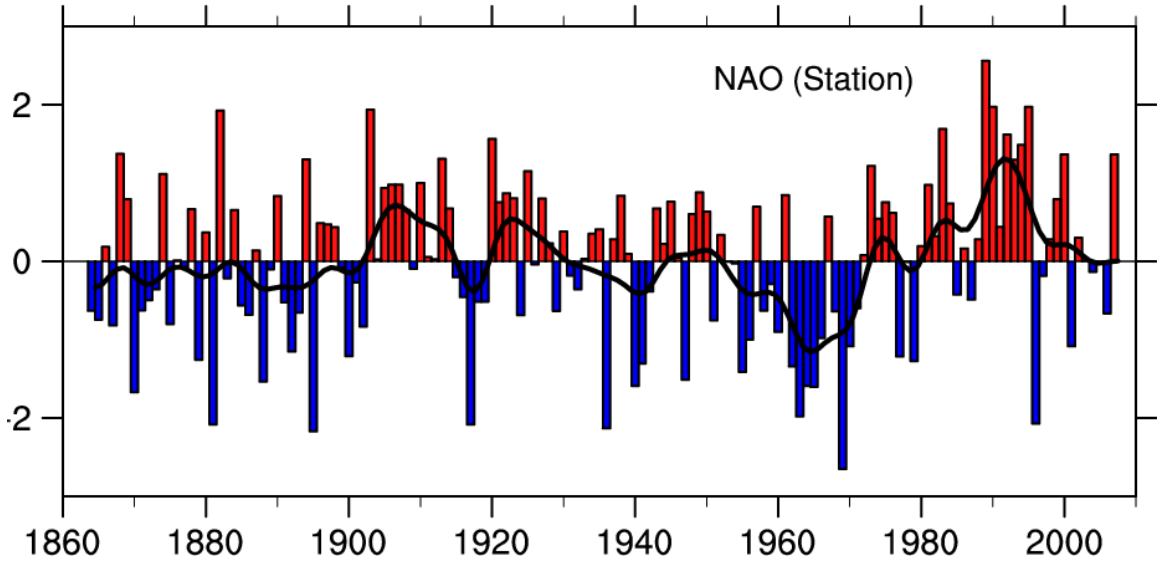

Figure 2.1. The boreal winter indices of the NAO that derived from difference in sea level pressure between Lisbon and Stykkisholmur. Here, the mean winter sea level pressure data at each station were normalized by division of each seasonal pressure by the long-term means (1864-1983) standard deviation. The heavy solid line represents the index smoothed to remove fluctuations with periods less than 4 years. The indicated year corresponds to the January of the winter season [2]. (taken from Hurrell et al., 2003).

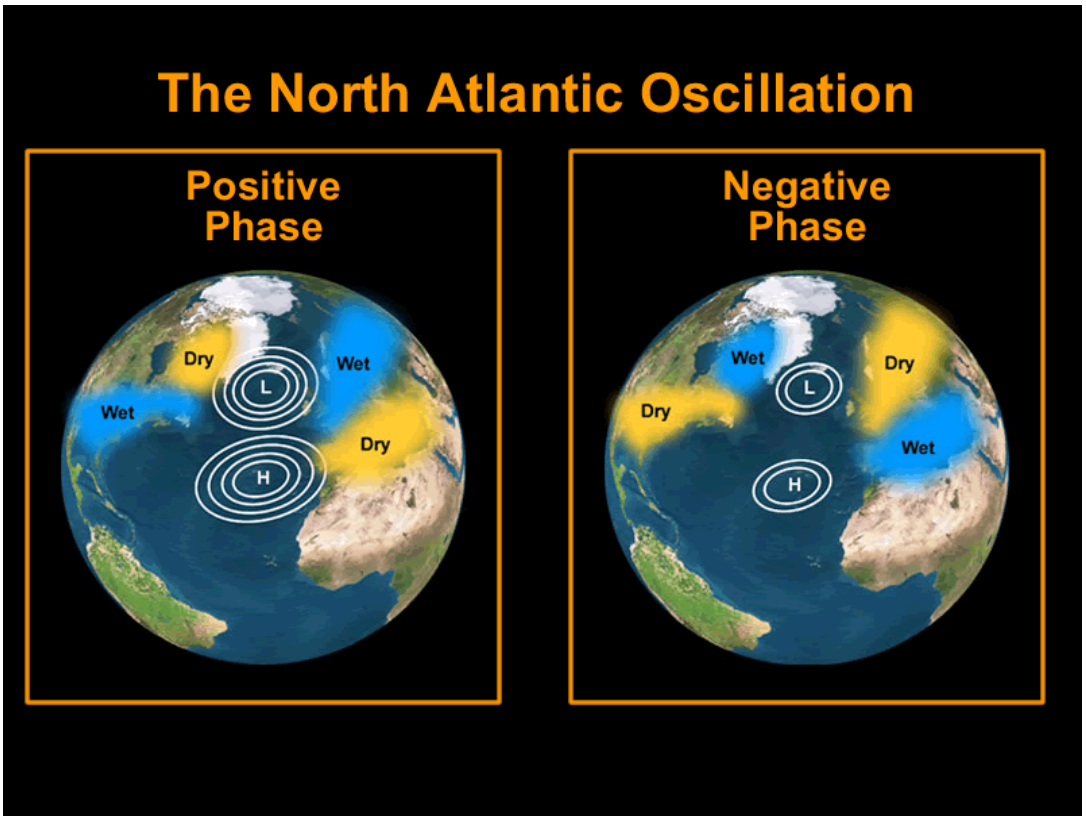

Figure 2.2. Positive and negative phases of the NAOI depending upon the dislocation of the northern low pressure center and the southern high pressure center [13, 14]. (courtesy of the University Corporation for Atmospheric Research-UCAR).

2.1.2. Impacts of the North Atlantic Oscillation

The North Atlantic Oscillation has a large climatic influence on the North Atlantic Ocean and surrounding land masses and it is a very important controlling factor in fundamental meteorological variables such as surface wind, temperature and precipitation which have large socio-economic impacts on energy, agriculture, industry, traffic and human health throughout the whole of Europe and eastern North America. The NAO shows a dominant influence mainly on wintertime temperature across much of the Northern Hemisphere (NH). The NAO variability is significantly correlated with the surface air temperature and sea surface temperature (SST) across the vast areas of the North Atlantic Ocean, the Arctic, the North America, the Mediterranean and Eurasia.

During high NAO years, winter temperatures are higher there than during years with a normal or low NAO [2].

Different phase situations (positive and negative) have different impacts upon the regions of the Northern Hemisphere (Figure 2.3. and Figure 2.4.). During the positive phase of the North Atlantic Oscillation, a large pressure gradient across the North Atlantic creates strong winds that drive winter storms across the Atlantic and into Northern Europe. During the negative phase, there is only a small pressure gradient. Southern Europe and Africa receive weak winter storms while Northern Europe and the eastern United States are cold and dry [2].

As is seen in Figure 2.2. and Figure 2.3., the positive NAO index phase shows a stronger than usual subtropical high pressure center and a deeper than normal Icelandic low. The increased pressure difference results in more and stronger winter storms crossing the Atlantic Ocean on a more northerly track. This results in warm and wet winters in Europe and in cold and dry winters in northern Canada and Greenland. The eastern US experiences mild and wet winter conditions [15, 16].

As is illustrated like in Figure 2.2. and Figure 2.4., the negative NAO index phase shows a weak subtropical high and a weak Icelandic low. The reduced pressure gradient results in fewer and weaker winter storms crossing on a more west-east pathway. They bring moist air into the Mediterranean and cold air to northern Europe. The US east coast experiences more cold air outbreaks and hence snowy weather conditions. Greenland, however, will have milder winter temperatures [15, 16].

During the positive phase of the NAOI, enhanced westerly flow across the North Atlantic during winter season moves relatively warm and moist maritime air over much of Europe and far downstream while stronger northerly winds over northeastern Canada and Greenland carry cold air southward and decrease land temperatures and also sea surface temperatures over the northwest Atlantic. Decadal changes in the North Atlantic atmospheric circulation in the form of the NAO results in the local cooling in the northwest Atlantic and the warming across Europe and downstream over Eurasia [2, 4, 11, 12].

The changes in the circulation patterns over the North Atlantic associated with the North Atlantic Oscillation cause the changes in the intensity and number of storms, their weather and the paths of them. By the way, the winters during positive NAO index usually are related with the northeastward shifts in the Atlantic storm activities [2, 11, 17].

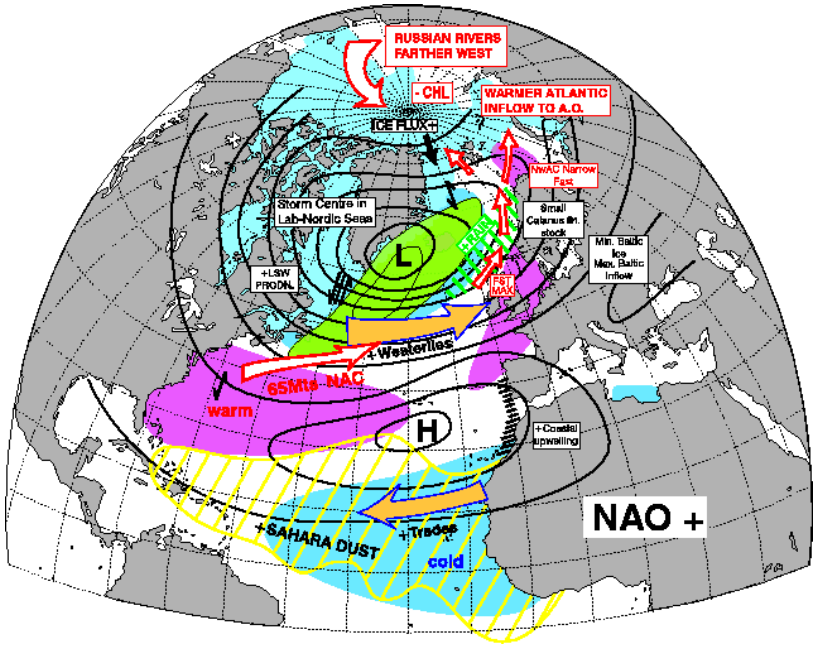

Figure 2.3. Positive phase of the NAOI. The major changes are seen on some regions in the NH related to the positive NAOI variability [15].

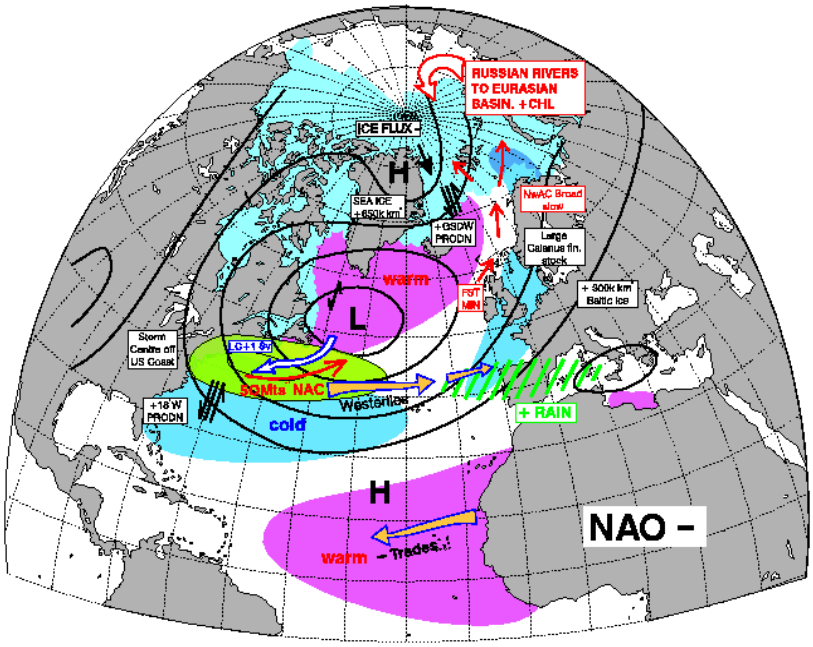

Figure 2.4. Negative phase of the NAOI. The major changes are seen on some regions in the NH related to the negative NAOI variability [15].

The swings of NAO indices are also associated with the changes in the mean flow and storminess. These changes are reflected in prominent variations in the transport of atmospheric moisture due to the distribution of evaporation and precipitation. During the winters with high NAO index, evaporation exceeds precipitation over the Canadian Arctic. More precipitation occurs than normal fall seasons from Iceland through Scandinavia, whereas drier conditions are seen over central and southern Europe, some parts of the Middle East and the Mediterranean [2, 18].

If we want to be more specific to understand better the effect of the NAO, we can obviously see local effects of the NAO. For instance, between the NAO and temperature, and sea level pressure in Israel there are statistically significant correlations [19]. Another study had showed that the temperature and the NAOI relationships were nearly linear especially in winter season over Europe [20]. According to Xoplaki, there are a high negative correlation between the winter (DJFM) NAOI and the winter Arctic Oscillation

indices, and winter air temperatures over a vast region (mainly mid-Algeria, Egypt, Libya, Cyprus, southern Italy, Greece and Turkey) [21]. Hasanean also revealed a high negative relationship between winter temperatures in Egypt and the winter NAOI [22]. Some researches have also done into see impacts of the NAO on Turkey. These recent studies show that the NAO has an important role on the spatial and temporal variability of the precipitation in Turkey [23, 24]. One of these recent studies revealed a negative relationship between year to year variability of the winter temperatures of Turkey and the winter NAOI. This result has a good agreement with the study done for Greece [25, 26]. During the weak phase of the NAOI winter composite temperatures in Turkey mostly increases, whereas it decreases during the strong phases of the NAOI [25].

2.2. Correlation Analysis

In the statistics, the correlation describes a linear statistical relationship between two random variables. Here, "linear statistical" refers the mean of one of the random variables is linearly dependent upon the random component of the other. The stronger linear relationship means the stronger correlation. Correlations manifest themselves in various ways in observed and simulated climates. Several adjectives are used to describe correlations depending upon whether they describe relationships in time (serial correlation, lagged correlation), space (spatial correlation) or between different climate variables (cross-correlation) [27, 28].

Correlation is represented by the correlation coefficients which vary between +1 and -1 and are independent of the units of measurement. A correlation coefficient of +1 (-1) indicates a pair of variables that vary together precisely, one variable being related to the other by means of positive (negative) scaling factor. The correlation coefficient is calculated by the equation written below (Equation 2.1.):

$$\rho_{XY} = \frac{\varepsilon((X - \mu_X)(Y - \mu_Y))}{\sigma_X \sigma_Y} \tag{2.1.}$$

In the Equation 2.1., the standard deviation $\sigma_X = \sqrt{Var(X)}$ and σ_Y is defined

analogously. *Var* means variance and it describes how far values lie from the mean. The correlation coefficient measures the tendency of X and Y to co-vary, so that the greater $|\rho|$, the greater the ability of X to specify Y. By the way, in the Equation 2.1., μ_X and μ_Y symbols are used to represent the mean of X and Y respectively. The expected values are shown by $\varepsilon(X)$ and $\varepsilon(Y)$. Note that σ_{XY} takes values in the range [-1, +1]. A value of ρ near 0 indicates little correlation between attributes; a value near +1 or -1 indicates a high level of correlation. When two attributes have a positive correlation coefficient, an increase in the value of one attribute indicates a likely increase in the value of the second attribute. A correlation coefficient of less than 0 indicates a negative correlation. That is, when one attribute shows an increase in value, the other attribute tends to show a decrease [27, 28].

2.3. The Correlation Analysis of Turkey's Precipitation and Temperature Data with the North Atlantic Oscillation Index

The most important variation of atmospheric mass, energy and momentum in the North Atlantic-European area in all seasons is associated with the North Atlantic Oscillation. As it has been mentioned before, the NAO also has influences on the climate of Turkey. The most of studies in the literature have been done for the winter seasons. In contradistinction to common researches, in this study annual data were used to see annual relationship between the North Atlantic Oscillation index and the variables of temperature and precipitation in Turkey.

First of all, two main climate parameters (precipitation and temperature) were chosen to contrast with the North Atlantic Oscillation indices. Observation values for each dataset were selected between January of 1980 and December of 2000.

There are 311 weather stations in Turkey and all these stations are situated randomly on different regions of the country. The weather stations in Turkey are illustrated on a geographical map in Figure 2.5.

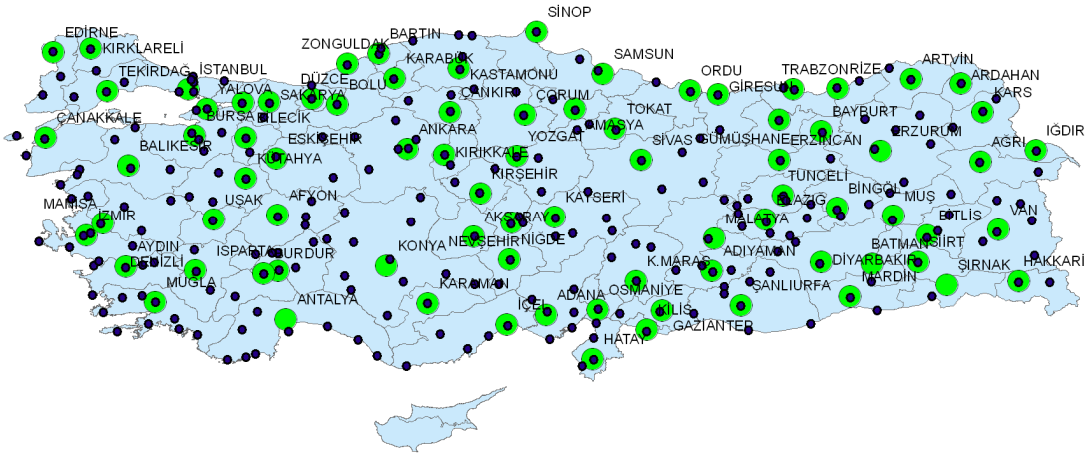

Figure 2.5. The weather stations in Turkey

.

150 stations were chosen among 311 weather stations to be used. There stations were chosen by taking notice of the most available dataset needed in study, so the locations of the stations were not considered. The map of selected weather stations is like shown in Figure 2.6.

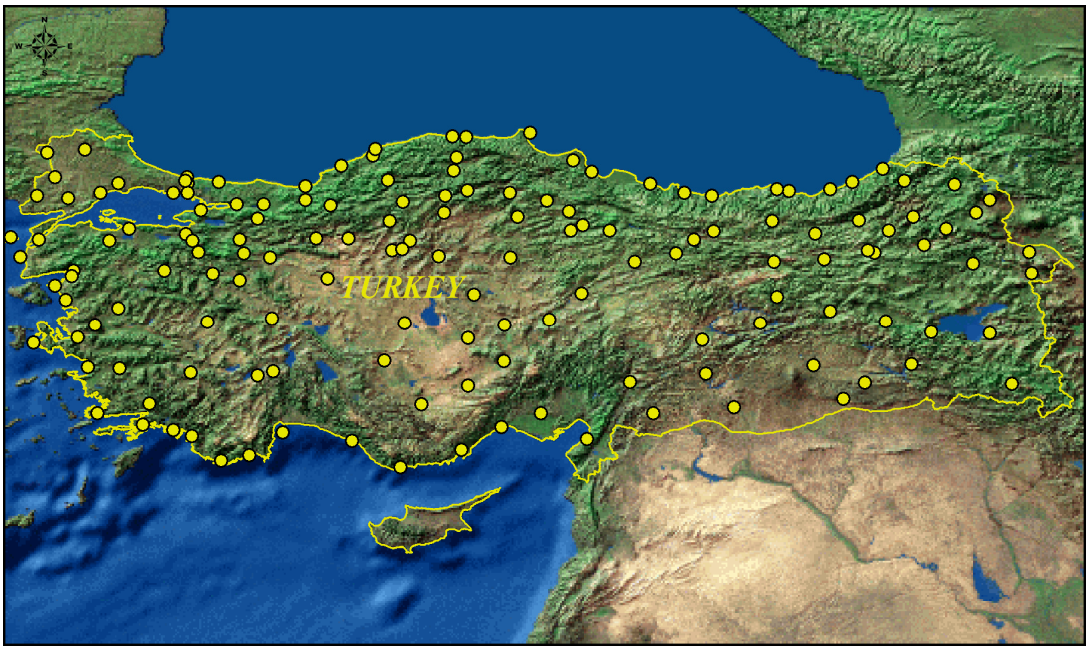

Figure 2.6. The map of the weather stations used in the research. Every point represents a station where it is located.

After the station selection, monthly mean temperature and precipitation records for each selected stations were chosen for the timescale from 1980's first month (January) to 2000's last month (December). Hence, each one of 150 stations were contained a dataset for 21 years. This means one station includes a dataset for 252 months. Table 2.1. shows the number of stations separated in reference to different seven geographical regions of Turkey.

Table 2.1. Regional Classification of Selected Weather Stations

REGION	NUMBER OF STATIONS
BLACK SEA	36
MARMARA	26
CENTRAL ANATOLIA	25
AEGEAN	22
MEDITERRANEAN	11
EASTERN ANATOLIA	23
SOUTHEAST ANATOLIA	7

According to Table 2.1., the most stations selected for study belong to Blacksea region of Turkey. 36 weather stations were selected from the northern side of Turkey Marmara region was come after Blacksea region which has 26 weather stations. As is ranked like in the Table 2.1., Southeast Anatolia region has got 7 stations and it is ranked as the last.

Table 2.2. shows all of the weather stations used in this research. Every station is identified with an international code called as "Station ID". The weather stations in Turkey are situated on unrelated places. Each one of the stations has different elevations like shown in Table 2.2. For example, the station in Sarıkamış is elevated 2102 meters from surface, whereas the station in Finike is elevated only 202 centimeters from surface.

Table 2.2. List of the Weather Stations Ranked by Station ID

STATION ID	STATION NAME	STATION REGION	ELEVATION (m)	LATITUDE (degree)	LONGITUDE (degree)
17020	BARTIN	BLACK SEA	32,52	41,63	32,34
17022	ZONGULDAK BOLGE	BLACK SEA	135,35	41,44	31,78
17024	INEBOLU	BLACK SEA	63,82	41,97	33,76
17026	SINOP	BLACK SEA	32,00	42,03	35,14
17030	SAMSUN BOLGE	BLACK SEA	4,00	41,34	36,24
17033	ORDU	BLACK SEA	4,13	40,97	37,89
17034	GIRESUN	BLACK SEA	38,00	40,91	38,38
17037	TRABZON BOLGE	BLACK SEA	30,00	40,59	39,45
17040	RIZE	BLACK SEA	8,60	41,03	40,49
17042	HOPA	BLACK SEA	32,56	41,39	41,43
17045	ARTVIN	BLACK SEA	628,35	41,18	41,81
17050	EDIRNE	MARMARA	51,19	41,68	26,54
17052	KIRKLARELI	MARMARA	231,50	41,73	27,21
17054	CORLU	MARMARA	183,00	41,14	27,81
17056	TEKIRDAG	MARMARA	3,60	40,97	27,49
17059	KUMKOY-KILYOS	MARMARA	38,18	41,24	29,03
17061	SARIYER-KIRECBURNU	MARMARA	58,54	41,14	29,04
17062	ISTANBUL BOLGE	MARMARA	32,98	40,97	29,04
17066	KOCAELI-IZMIT	MARMARA	76,00	40,76	29,91
17069	SAKARYA-ADAPAZARI	MARMARA	30,43	40,76	30,39
17070	BOLU	BLACK SEA	742,92	40,74	31,59
17072	DUZCE	BLACK SEA	145,67	40,84	31,14
17074	KASTAMONU	BLACK SEA	799,91	41,36	33,78

Table 2.3. Continuation of Table 2.2.

STATION ID	STATION NAME	STATION REGION	ELEVATION (m)	LATITUDE (degree)	LONGITUDE (degree)
17078	KARABUK	BLACK SEA	259,31	41,19	32,61
17080	CANKIRI	CENTRAL ANATOLIA	751,00	40,61	33,61
17083	MERZIFON	BLACK SEA	544,00	40,83	35,44
17084	CORUM	BLACK SEA	775,91	40,54	34,92
17085	AMASYA	BLACK SEA	411,69	40,64	35,84
17086	TOKAT BOLGE	BLACK SEA	607,60	40,29	36,56
17088	GUMUSHANE	BLACK SEA	1219,00	40,46	39,46
17090	SIVAS	CENTRAL ANATOLIA	1285,00	39,74	37,01
17094	ERZINCAN	EASTERN ANATOLIA	1218,22	39,74	39,49
17096	ERZURUM MEYDAN	EASTERN ANATOLIA	1758,18	39,94	41,16
17097	KARS BOLGE	EASTERN ANATOLIA	1775,00	40,61	43,09
17099	AGRI	EASTERN ANATOLIA	1632,00	39,71	43,04
17100	IGDIR	EASTERN ANATOLIA	858,00	39,91	44,04
17110	GOKCEADA	MARMARA	79,00	40,18	25,89
17111	BOZCAADA	AEGEAN	30,00	39,83	26,06
17112	CANAKKALE	MARMARA	5,50	40,13	26,39
17114	BANDIRMA	MARMARA	63,00	40,33	28,00
17116	BURSA	MARMARA	100,32	40,23	29,01
17095	ERZURUM BOLGE	EASTERN ANATOLIA	1869,00	39,54	41,17
17119	YALOVA	MARMARA	3,81	40,66	29,28
17120	BILECIK	MARMARA	539,19	40,14	29,97
17123	ESKISEHIR ANADOLU	CENTRAL ANATOLIA	787,00	39,81	30,51
17128	ESENBOGA MEYDAN	CENTRAL ANATOLIA	959,33	40,11	33,00
17129	ETIMESGUT MEYDAN	CENTRAL ANATOLIA	806,15	39,94	32,68
17130	ANKARA BOLGE	CENTRAL ANATOLIA	890,52	39,96	32,86
17135	KIRIKKALE	CENTRAL ANATOLIA	750,89	39,84	33,51

Table 2.4. Continuation of Table 2.2.

STATION ID	STATION NAME	STATION REGION	ELEVATION (m)	LATITUDE (degree)	LONGITUDE (degree)
17140	YOZGAT	CENTRAL ANATOLIA	1298,43	39,81	34,79
17145	EDREMIT	AEGEAN	20,66	39,58	27,01
17155	KUTAHYA	AEGEAN	969,28	39,41	29,97
17160	KIRSEHIR BOLGE	CENTRAL ANATOLIA	1007,17	39,16	34,14
17162	GEMEREK	CENTRAL ANATOLIA	1171,00	39,18	36,06
17165	TUNCELI	EASTERN ANATOLIA	980,91	39,11	39,54
17172	VAN BOLGE	EASTERN ANATOLIA	1670,52	38,46	43,34
17175	AYVALIK	AEGEAN	3,55	39,31	26,68
17180	DIKILI	AEGEAN	3,40	39,06	26,87
17184	AKHISAR	AEGEAN	92,03	38,91	27,81
17186	MANISA	AEGEAN	71,00	38,61	27,39
17188	USAK	AEGEAN	919,22	38,66	29,39
17190	A.KARAHİSAR BOLGE	AEGEAN	1033,74	38,73	30,54
17191	CIHANBEYLI	CENTRAL ANATOLIA	968,73	38,64	32,91
17192	AKSARAY	CENTRAL ANATOLIA	960,77	38,38	34,04
17193	NEVSEHIR	CENTRAL ANATOLIA	1259,54	38,61	34,69
17196	KAYSERI BOLGE	CENTRAL ANATOLIA	1092,00	38,71	35,48
17199	MALATYA BOLGE	EASTERN ANATOLIA	947,87	38,34	38,21
17201	ELAZIG BOLGE	EASTERN ANATOLIA	989,75	38,64	39,24
17203	BINGOL	EASTERN ANATOLIA	1177,00	38,86	40,49
17204	MUS	EASTERN ANATOLIA	1322,76	38,68	41,48
17205	TATVAN	EASTERN ANATOLIA	1664,65	38,48	42,29
17210	SIIRT	SOUTHEAST ANATOLIA	895,54	37,91	41,94
17220	IZMIR BOLGE	AEGEAN	28,55	38,39	27,08
17221	CESME	AEGEAN	5,00	38,29	26,29

Table 2.5. Continuation of Table 2.2.

STATION ID	STATION NAME	STATION REGION	ELEVATION (m)	LATITUDE (degree)	LONGITUDE (degree)
17232	KUSADASI	AEGEAN	25,00	37,86	27,26
17234	AYDIN	AEGEAN	56,30	37,83	27,83
17237	DENIZLI	AEGEAN	425,29	37,76	29,09
17238	BURDUR	MEDITERRANEAN	957,00	37,71	30,29
17240	ISPARTA BOLGE	MEDITERRANEAN	996,88	37,78	30,56
17244	KONYA MEYDAN	CENTRAL ANATOLIA	1030,61	37,97	32,54
17246	KARAMAN	CENTRAL ANATOLIA	1023,05	37,19	33,21
17248	EREGLI-KONYA	CENTRAL ANATOLIA	1042,00	37,53	34,04
17250	NIGDE	CENTRAL ANATOLIA	1210,50	37,96	34,68
17255	K.MARAS	EASTERN ANATOLIA	572,13	37,59	36,92
17261	GAZIANTEP	SOUTHEAST ANATOLIA	854,00	37,04	37,34
17265	ADIYAMAN	SOUTHEAST ANATOLIA	672,00	37,74	38,28
17270	SANLIURFA BOLGE	SOUTHEAST ANATOLIA	547,19	37,14	38,78
17275	MARDIN	SOUTHEAST ANATOLIA	1050,00	37,29	40,73
17280	DIYARBAKIR MEYDAN	SOUTHEAST ANATOLIA	674,01	37,89	40,19
17282	BATMAN	SOUTHEAST ANATOLIA	610,00	37,58	41,11
17285	HAKKARI	EASTERN ANATOLIA	1727,74	37,56	43,73
17290	BODRUM	AEGEAN	26,47	37,03	27,43
17292	MUGLA	AEGEAN	646,07	37,21	28,36
17294	DALAMAN	AEGEAN	13,00	36,74	28,78
17296	FETHIYE	AEGEAN	3,00	36,63	29,11
17298	MARMARIS	AEGEAN	16,19	36,83	28,24
17300	ANTALYA MEYDAN	MEDITERRANEAN	63,57	36,69	30,73
17310	ALANYA	MEDITERRANEAN	5,88	36,54	31,97
17320	ANAMUR	MEDITERRANEAN	3,94	36,08	32,83

Table 2.6. Continuation of Table 2.2.

STATION ID	STATION NAME	STATION REGION	ELEVATION (m)	LATITUDE (degree)	LONGITUDE (degree)
17330	SILIFKE	MEDITERRANEAN	15,01	36,38	33,92
17340	MERSIN	MEDITERRANEAN	3,40	36,79	34,63
17351	ADANA BOLGE	MEDITERRANEAN	27,00	37,04	35,34
17370	ISKENDERUN	MEDITERRANEAN	3,59	36,58	36,16
17375	FINIKE	MEDITERRANEAN	2,02	36,29	30,14
17380	KAS-ANTALYA	MEDITERRANEAN	153,39	36,19	29,64
17602	AMASRA	BLACK SEA	73,00	41,74	32,38
17606	BOZKURT	BLACK SEA	167,00	41,96	34,00
17608	UZUNKOPRU	MARMARA	51,69	41,24	26,68
17610	SILE	MARMARA	83,00	41,16	29,59
17612	AKCAKOCA	BLACK SEA	10,00	41,08	31,14
17618	DEVREKANI	BLACK SEA	1050,00	41,59	33,83
17619	BAHCEKOY OR.FAK.	MARMARA	129,63	41,18	29,00
17622	BAFRA	BLACK SEA	103,00	41,54	35,91
17624	UNYE	BLACK SEA	20,00	41,13	37,28
17626	AKCAABAT	BLACK SEA	6,00	41,03	39,54
17628	PAZAR-RIZE	BLACK SEA	79,00	41,16	40,89
17630	ARDAHAN	EASTERN ANATOLIA	1829,00	41,11	42,71
17632	IPSALA	MARMARA	9,71	40,91	26,36
17634	MALKARA	MARMARA	207,00	40,87	26,91
17636	FLORYA	MARMARA	37,20	40,97	28,78
17646	CERKES	BLACK SEA	1126,00	40,81	32,87
17648	ILGAZ	CENTRAL ANATOLIA	885,00	40,91	33,63
17650	TOSYA	BLACK SEA	870,00	41,01	34,03
17652	OSMANCIK	BLACK SEA	419,00	40,97	34,78

Table 2.7. Continuation of Table 2.2.

STATION ID	STATION NAME	STATION REGION	ELEVATION (m)	LATITUDE (degree)	LONGITUDE (degree)
17656	ARPACAY	EASTERN ANATOLIA	1688,00	40,84	43,33
17662	GEYVE[A.F.P.]	MARMARA	100,00	40,51	30,29
17664	KIZILCAHAMAM	CENTRAL ANATOLIA	1033,00	40,46	32,64
17666	ISPIR	EASTERN ANATOLIA	1222,00	40,48	41,00
17668	OLTU	EASTERN ANATOLIA	1322,00	40,54	41,97
17674	GONEN	MARMARA	37,00	40,11	27,64
17676	ULUDAG-ZIRVE	MARMARA	1877,00	40,11	29,13
17679	NALLIHAN	CENTRAL ANATOLIA	650,00	40,16	31,33
17680	BEYPAZARI	CENTRAL ANATOLIA	682,00	40,16	31,91
17681	ZILE	BLACK SEA	717,00	40,29	35,87
17682	SEBINKARAHISAR	BLACK SEA	1364,00	40,28	38,41
17683	TURHAL	BLACK SEA	529,73	40,39	36,08
17684	SUSEHRI	CENTRAL ANATOLIA	1163,00	40,14	38,06
17686	BAYBURT	BLACK SEA	1584,00	40,24	40,23
17688	TORTUM	BLACK SEA	1572,00	40,29	41,54
17690	HORASAN	EASTERN ANATOLIA	1540,00	40,04	42,16
17692	SARIKAMIS	EASTERN ANATOLIA	2102,00	40,33	42,56
17695	KELES	MARMARA	1063,00	39,91	29,23
17700	DURSUNBEY	AEGEAN	637,00	39,58	28,63
17702	BOZUYUK	MARMARA	754,00	39,89	30,04
17704	TAVSANLI	AEGEAN	833,00	39,53	29,49
17716	ZARA	CENTRAL ANATOLIA	1347,00	39,89	37,74
17718	TERCAN	EASTERN ANATOLIA	1425,00	39,78	40,38
17720	DOGUBEYAZIT	EASTERN ANATOLIA	1725,00	39,54	44,08
17722	BURHANIYE	AEGEAN	20,00	39,49	26,97
17726	SIVRIHISAR	CENTRAL ANATOLIA	1070,00	39,44	31,53

Before we got started to determine the relationship between the North Atlantic Oscillation and the climatic variables (temperature and precipitation) of Turkey, the NAOI were chosen in the same time range (from January-1980 to December-2000) with the station records. The station based monthly indices were preferred to perform correlation analysis. Monthly index of the NAO based on the difference of normalized sea level pressures between Ponta Delgada, Azores and Stykkisholmur in Reykjavik, Iceland since 1865. We just used the indices for a period from the beginning of 1980 to the end of 2000. Figure 2.7. draws a timeseries graph of the NAOI between 1980-October and 2000-December. The NAOI vary between the positive and negative values. The entire dataset includes 252 index values. 110 values of total 252 are negative, whereas the rest of them are positive. This means the NAO was in its weak phase for 110 months and 142 months of this period were showed the strong NAO. For example, the North Atlantic Oscillation was so strong on October of 2000. The NAO index is + 4.5 (mbar or hPa) for this month. On December in 1995, the NAO index is – 3.8 mbar and so the NAO is in its negative phase.

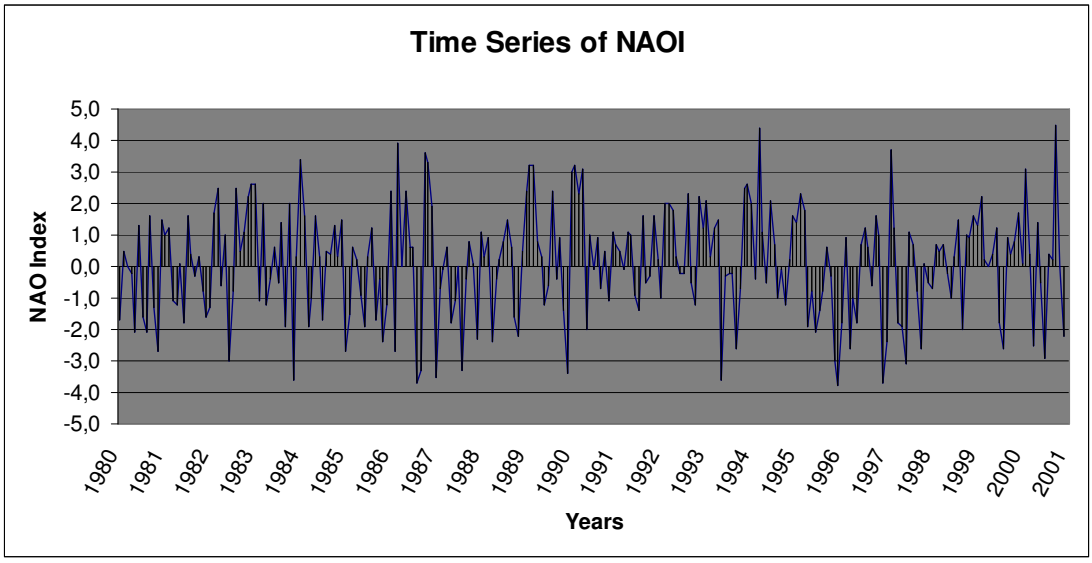

Figure 2.7. Time series of the NAOI between 1980 and 2001. Here, the monthly NAO indices that derived from difference in sea level pressure between Azores and Stykkisholmur.

Then by available data were supplied, the correlation coefficients were computed one by one for each one of the stations. The correlation coefficients were calculated by use of the Equation 2.1. hereinbefore. In Table 2.8., the correlation coefficients of every single stations are shown. First column in the Table 2.8. includes the correlation coefficients between the NAOI and precipitation. As is seen from the Table 2.8., much as some stations acted unequal, most of them got predominantly inverse correlation with the NAOI. A weak correlation was seen between the NAOI and precipitation. 126 stations have an inverse correlation with the NAOI. Some of the correlations coefficients for precipitation are almost zero. The highest correlation coefficients (above 0.2) are found in Ankara and Esenboğa Meydan, Etimesgut Meydan, Ankara Bölge, Kırıkkale, Devrekanı, Ilgaz, Tosya, Osmancık, Kızılcahamam, Nallıhan, Beypazarı, Sivrihisar (yellow cells in Table 2.8). While the central Anatolia and the western Blacksea regions give the better results, the eastern Anatolia and the southeast Anatolia have weaker correlations for precipitation.

The correlation analysis of temperature and the NAOI gave us the better and consistent results. The same correlation analysis was applied for temperature. As is seen from Table 2.8., it is obvious that there is an inverse correlation between the NAOI and the temperature of Turkey. All of the stations gave us negative correlation coefficients. Even though the correlation coefficients are not statistically strong enough, the results are coherent. The correlation coefficient between the NAOI and temperature is approximately at a level of 0.20 and it is negative.

Table 2.8. Correlation Coefficients

STATION ID	STATION NAME	PRECIPITATION & NAOI	TEMPERATURE & NAOI
17020	BARTIN	-0.03	-0.20
17022	ZONGULDAK BOLGE	-0.05	-0.19
17024	INEBOLU	-0.07	-0.19
17026	SINOP	-0.06	-0.18
17030	SAMSUN BOLGE	-0.15	-0.19
17033	ORDU	-0.06	-0.20
17034	GIRESUN	-0.05	-0.20
17037	TRABZON BOLGE	-0.04	-0.21
17040	RIZE	-0.05	-0.21
17042	HOPA	-0.06	-0.22
17045	ARTVIN	0.07	-0.22
17050	EDIRNE	-0.08	-0.16
17052	KIRKLARELI	-0.09	-0.17
17054	CORLU	-0.07	-0.17
17056	TEKIRDAG	-0.06	-0.17
17059	KUMKOY-KILYOS	-0.05	-0.17
17061	SARIYER-KIRECBURNU	-0.10	-0.17
17062	ISTANBUL BOLGE	-0.10	-0.18
17066	KOCAELI-IZMIT	-0.09	-0.19
17069	SAKARYA-ADAPAZARI	-0.06	-0.19
17070	BOLU	-0.19	-0.20
17072	DUZCE	-0.09	-0.20
17074	KASTAMONU	-0.26	-0.19
17078	KARABUK	-0.15	-0.20
17080	CANKIRI	-0.22	-0.19
17083	MERZIFON	-0.24	-0.20
17084	CORUM	-0.23	-0.21
17085	AMASYA	-0.21	-0.20
17086	TOKAT BOLGE	-0.18	-0.21
17088	GUMUSHANE	-0.16	-0.22

Table 2.9. Continuation of Table 2.8.

STATION ID	STATION NAME	PRECIPITATION & NAOI	TEMPERATURE & NAOI
17090	SIVAS	-0.15	-0.22
17094	ERZINCAN	-0.13	-0.21
17096	ERZURUM MEYDAN	-0.05	-0.21
17097	KARS BOLGE	-0.06	-0.23
17099	AGRI	-0.11	-0.24
17100	IGDIR	-0.03	-0.25
17110	GOKCEADA	0.01	-0.23
17111	BOZCAADA	-0.0045	-0.17
17112	CANAKKALE	0.02	-0.16
17114	BANDIRMA	0.01	-0.18
17116	BURSA	-0.06	-0.18
17095	ERZURUM BOLGE	-0.09	-0.19
17119	YALOVA	-0.13	-0.19
17120	BILECIK	-0.14	-0.20
17123	ESKISEHIR ANADOLU	-0.18	-0.19
17128	ESENBOGA MEYDAN	-0.25	-0.20
17129	ETIMESGUT MEYDAN	-0.26	-0.19
17130	ANKARA BOLGE	-0.25	-0.20
17135	KIRIKKALE	-0.24	-0.20
17140	YOZGAT	-0.17	-0.21
17145	EDREMIT	-0.05	-0.19
17155	KUTAHYA	-0.18	-0.20
17160	KIRSEHIR BOLGE	-0.21	-0.21
17162	GEMEREK	-0.18	-0.21
17165	TUNCELI	-0.10	-0.19
17172	VAN BOLGE	0.06	-0.22
17175	AYVALIK	0.03	-0.19
17180	DIKILI	-0.0069	-0.19
17184	AKHISAR	-0.02	-0.19
17186	MANISA	0.02	-0.19

Table 2.10. Continuation of Table 2.8.

STATION ID	STATION NAME	PRECIPITATION & NAOI	TEMPERATURE & NAOI
17188	USAK	-0.11	-0.19
17190	A.KARAHİSAR BOLGE	-0.15	-0.20
17191	CIHANBEYLI	-0.17	-0.21
17192	AKSARAY	-0.15	-0.21
17193	NEVSEHIR	-0.06	-0.22
17196	KAYSERI BOLGE	-0.08	-0.21
17199	MALATYA BOLGE	-0.03	-0.20
17201	ELAZIG BOLGE	-0.05	-0.20
17203	BINGOL	-0.02	-0.21
17204	MUS	0.06	-0.23
17205	TATVAN	-0.0020	-0.22
17210	SIIRT	-0.04	-0.19
17220	IZMIR BOLGE	0.05	-0.19
17221	CESME	0.04	-0.19
17232	KUSADASI	0.08	-0.19
17234	AYDIN	0.03	-0.19
17237	DENIZLI	-0.09	-0.19
17238	BURDUR	-0.15	-0.19
17240	ISPARTA BOLGE	-0.09	-0.19
17244	KONYA MEYDAN	-0.18	-0.21
17246	KARAMAN	-0.02	-0.22
17248	EREGLI-KONYA	-0.06	-0.22
17250	NIGDE	-0.11	-0.21
17255	K.MARAS	-0.04	-0.18
17261	GAZIANTEP	-0.04	-0.19
17265	ADIYAMAN	-0.04	-0.18
17270	SANLIURFA BOLGE	-0.06	-0.19
17275	MARDIN	-0.07	-0.20
17280	DIYARBAKIR MEYDAN	-0.02	-0.19
17282	BATMAN	-0.08	-0.20

Table 2.11. Continuation of Table 2.8.

STATION ID	STATION NAME	PRECIPITATION & NAOI	TEMPERATURE & NAOI
17285	HAKKARI	0.07	-0.19
17290	BODRUM	0.05	-0.19
17292	MUGLA	0.0016	-0.18
17294	DALAMAN	0.02	-0.18
17296	FETHIYE	0.03	-0.19
17298	MARMARIS	0.02	-0.18
17300	ANTALYA MEYDAN	-0.02	-0.19
17310	ALANYA	-0.02	-0.19
17320	ANAMUR	0.01	-0.19
17330	SILIFKE	0.02	-0.18
17340	MERSIN	-0.0072	-0.19
17351	ADANA BOLGE	-0.01	-0.18
17370	ISKENDERUN	-0.08	-0.19
17375	FINIKE	0.02	-0.19
17380	KAS-ANTALYA	0.02	-0.22
17602	AMASRA	-0.05	-0.41
17606	BOZKURT	-0.07	-0.19
17608	UZUNKOPRU	-0.05	-0.17
17610	SILE	-0.12	-0.17
17612	AKCAKOCA	-0.05	-0.20
17618	DEVREKANI	-0.26	-0.22
17619	BAHCEKOY OR.FAK.	-0.07	-0.18
17622	BAFRA	-0.15	-0.19
17624	UNYE	-0.15	-0.19
17626	AKCAABAT	-0.03	-0.20
17628	PAZAR-RIZE	-0.03	-0.22
17630	ARDAHAN	-0.14	-0.24
17632	IPSALA	0.0040	-0.16
17634	MALKARA	-0.04	-0.17
17636	FLORYA	-0.09	-0.17

Table 2.12. Continuation of Table 2.8.

STATION ID	STATION NAME	PRECIPITATION & NAOI	TEMPERATURE & NAOI
17646	CERKES	-0.19	-0.20
17648	ILGAZ	-0.22	-0.19
17650	TOSYA	-0.27	-0.18
17652	OSMANCIK	-0.28	-0.19
17656	ARPACAY	-0.13	-0.23
17662	GEYVE[A.F.P.]	-0.06	-0.19
17664	KIZILCAHAMAM	-0.20	-0.20
17666	ISPIR	-0.10	-0.21
17668	OLTU	-0.11	-0.22
17674	GONEN	-0.05	-0.19
17676	ULUDAG-ZIRVE	-0.02	-0.19
17679	NALLIHAN	-0.20	-0.18
17680	BEYPAZARI	-0.24	-0.18
17681	ZILE	-0.19	-0.22
17682	SEBINKARAHISAR	-0.12	-0.21
17683	TURHAL	-0.18	-0.20
17684	SUSEHRI	-0.11	-0.21
17686	BAYBURT	-0.11	-0.23
17688	TORTUM	-0.10	-0.22
17690	HORASAN	-0.04	-0.24
17692	SARIKAMIS	-0.08	-0.23
17695	KELES	-0.10	-0.20
17700	DURSUNBEY	-0.08	-0.20
17702	BOZUYUK	-0.10	-0.20
17704	TAVSANLI	-0.18	-0.20
17716	ZARA	-0.18	-0.22
17718	TERCAN	-0.09	-0.22
17720	DOGUBEYAZIT	0.07	-0.23
17722	BURHANIYE	-0.06	-0.19
17726	SIVRIHISAR	-0.20	-0.19

3. PREDICTION OF THE NORTH ATLANTIC OSCILLATION INDICES IN FUTURE BY USING COMPUTATIONAL AND STATISTICAL METHODS

3.1. Regression Analysis

In statistics, regression analysis includes any techniques for modeling and analyzing several variables, when the focus is on the relationship between a dependent variable and one or more independent variables. More specifically, regression analysis helps us understand how the typical value of the dependent variable changes when any one of the independent variables is varied, while the other independent variables are held fixed. Regression is very similar to correlation, but instead of measuring the relationship it provides to make predictions based on the relationship, so that regression analysis is widely used for prediction and forecasting. Regression analysis is also used to understand which among the independent variables are related to the dependent variable, and to explore the forms of these relationships. In restricted circumstances, regression analysis can be used to infer causal relationships between the independent and dependent variables. Even though we do not infer a causal relationship, we can nevertheless predict one variable if we have information about the other. If we assume X as the predictor variable and Y as the criterion variable, we can attempt to use X in order to predict what Y should be [27, 28, 29, 30].

In regression analysis, first of all the best fitting line for the data is computed by drawing a line at a scatter plot to indicate the direction of the effect. In a scatter plot a single line does not hit every data point, but we can construct a line that simultaneously comes as close to each data point as possible.

As with similar topics in geometry, we express the line we come up with in an equation. Recognize that the Equation 3.1.:

$$Y = mx + b \tag{3.1.}$$

In regression analysis, a similar equation (Equation 3.2.) is used to express a straight line:

$$\hat{Y} = bX + a \tag{3.2.}$$

Even though we use "b" here, it is still the slope of the line, and "a" is the y-intercept. In the Equation 3.2. $\hat{Y}$ is also used instead of just Y to indicate that this is a predicted value for way based on the regression line rather then an actual Y-value. In order to make predictions, these regression coefficients (b and a) must be computed and plugged into the equation. We can then plug in an X-value and get out a predicted Y value ($\hat{Y}$) [27, 28, 29, 30].

Slope is the unit change in Y for each single unit change in X. That is, since we multiply the slope with the X-value we want to make predictions about, the predicted Y changes by the amount of the slope for each single unit of X. Slope computation is very similar to correlation (Equation 3.3.). In fact, if the correlation has already been computed the same values can be used to compute slope [27, 28, 29, 30].

$$b = \frac{\sum XY - \frac{\sum X \sum Y}{n}}{\sum X^2 - \frac{(\sum X)^2}{n}} \tag{3.3.}$$

Notice that we have the covariation of X and Y in the numerator, so the entire numerator will be the same as with ρ . The denominator is the sums of squares for X. This is a portion of the denominator for ρ as well [27, 28, 29, 30].

The y-intercept is the point at which the regression line crosses the Y-axis. It is also the value we predict for Y when X = 0. That is because we are at the Y-axis when X=0. In Equation 3.4. notice that we must compute the slope "b" before we can compute the y-intercept [27, 28, 29, 30].

$$a = \frac{\sum Y - b\sum X}{n} \tag{3.4.}$$

3.2. Climate Modelling

Climate models are mathematical models constructed to analyze atmospheric and climatic parameters such as surface pressure, surface temperature, ocean surface temperature, ocean surface pressure, precipitation, near surface wind, surface sensible heat flux, radiation, etc. They include the effects of oceans, whereas weather forecasting models do not. These models require feedbacks (water vapour feedback, cloud-radiation feedback, ocean circulation feedback and ice-albedo feedback), atmosphere ocean interactions and different greenhouse gas emission scenarios. More than 15 research centers in the world in 10 countries are currently running climate models [31, 32].

Before the model can be used for prediction it has to be run for a considerable time until it reaches steady climate. Once a comprehensive climate model has been formulated it can be tested in three main ways. Firstly, it can be run for a number of years of simulated time and the climate generated by the model compared in detail to the current climate. For the model to be seen as a valid one, the average distribution and the seasonal variations of appropriate parameters such as surface pressure, temperature and precipitation have to compare well with observation. In the same way, the variability of the model's climate must be similar to the observed variability. Climate models that are currently employed for climate prediction stand up well to such comparisons [31].

Secondly, models can be compared against simulations of past climates when the distribution of key variables was substantially different than at present [31].

A third way in which models can be validated is to use them to predict the effect of large perturbations on the climate. Good progress is being achieved with the prediction of El Nino events and the associated climate anomalies up to year ahead [31].

Climate models are systems of differential equations based on the basic laws of physics, fluid motion, and chemistry. To run a model, scientists divide the planet into a 3-dimensional grid (Figure 3.1. – courtesy of the NOAA), apply the basic equations, and evaluate the results [31, 32].

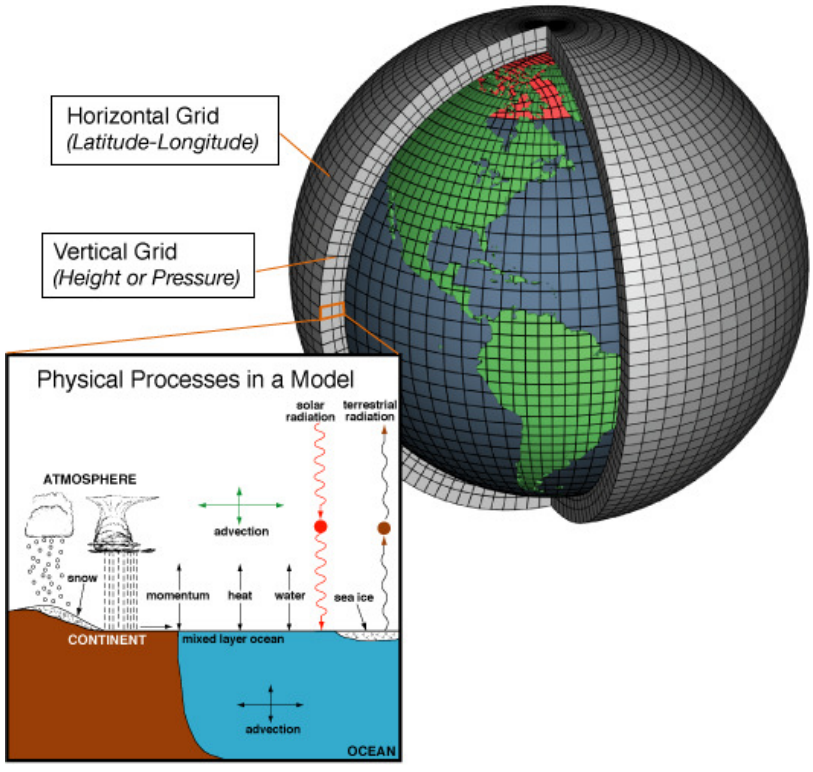

Figure 3.1. Atmospheric Model Schematic

Global models with grid resolution of about 300 km in the horizontal are called "General Circulation Models or Global Climate Models (GCMs)". GCMs try to simulate as much as possible about the climate system such as the incoming and outgoing radiation, the way the air moves, the way clouds form and precipitation falls, the way the ice sheets grow or shrink, etc [31, 32, 33].

Weather and climate on scales large compared with the grid size are described reasonably well. However, at scales comparable with the grid size, described as the regional scale (the regional scale is defined as describing the range of 10^4 to 10^7 km^2), the results from global models possess serious limitations. The effects of forcing and circulations that exist on the regional scale need to be properly represented. For example, patterns of precipitation depend critically on the major variations in orography and surface characteristics that occur on this scale. Patterns generated by a global model therefore will be a poor representation of what actually occurs on the regional scale [31, 32, 33].

To overcome these limitations regional modelling techniques have been developed. That most readily applicable to climate simulation and prediction is the "Regional Climate Model (RCM). A model covering an appropriate region at a horizontal resolution of say 25 or 50 km can be nested in a global model [Figure 3.2. - courtesy of the climateprediction.net]. The global model provides information about the response of the global circulation to large-scale forcings and the evolution of the boundary information for RCM. Within the region, physical information, for instance concerning forcings, is entered on the scale of the regional grid and the evolution of the detailed circulation is developed within the RCM. The RCM is able to account for forcings due to topography or land cover inhomogeneity on smaller scales than are included in the GCM and it can also simulate atmospheric circulations and climate variables on these smaller scales. The Regional Climate Models can resolve the local impacts given small scale information about orography, land use etc., giving weather and climate information at resolutions as fine as 50 or 25 km. Figure 3.3. shows that winter precipitation over Britain as predicted by a) a GCM with resolution 300km, b) a regional model with 50km resolution and c) a regional model with 25km resolution compared to d) actual observations.

There is also a limitation for the RCM. The RCM does not provide interaction back on to the GCM, although the GCM provides the boundary inputs for the RCM [31, 32, 33, 34].

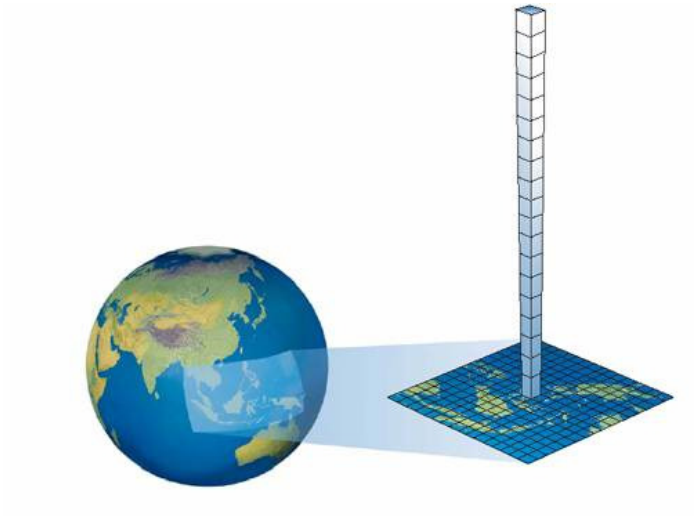

Figure 3.2. The vertical and horizontal grids of the RCMs.

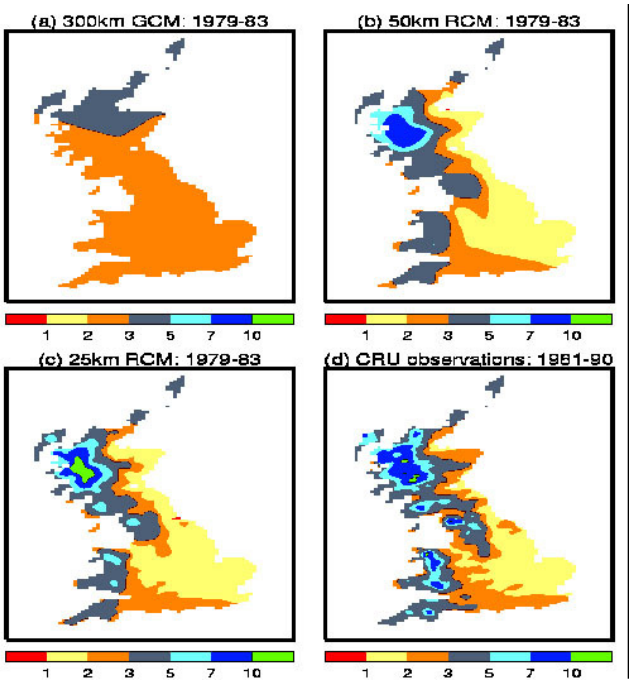

Figure 3.3. Prediction of winter precipitation over Britain in different resolutions.

3.2.1. Model RegCM – 4.0

RegCM – 4.0 (the newest version) was used in this study, which is a regional climate model developed by Abdus Salam International Centre for Theoretical Physics (ICTP). The Regional Climate Model (RegCM) is a three dimensional, sigma-coordinate, primitive equation regional climate model. The RegCM modeling system has four components: Terrain, ICBC (initial conditions and boundary conditions), RegCM and Postprocessor. Terrain and ICBC are the two components of RegCM preprocessor. Terrestrial variables (including elevation, land use and sea surface temperature) and three-dimensional isobaric meteorological data are horizontally interpolated from a latitude-longitude mesh to a high-resolution domain on either a Rotated (and Normal) Mercator, Lambert Conformal, or Polar Stereographic projection. Vertical interpolation from pressure levels to the sigma coordinate system of RegCM is also performed. Sigma surfaces near the ground closely follow the terrain, and the higher-levels surfaces tend to approximate isobaric surfaces. After doing necessary parameterization in the programme, the model can be run for any domain with any grid numbers in available resolutions [35, 36].

3.3. Prediction of the North Atlantic Oscillation Indices Due to Temperature and Precipitation Variables

In this part of study, the North Atlantic Oscillation indices in future were predicted. Model results were used to estimate the NAOI. A decade term between 1990 and 2000 was taken as a basis and two terms (2040-2050 and 2090-2100) were also chosen for future predictions.

Firstly, the RegCM-4.0 was run for with a grid resolution in 40 km for the domain of Turkey including some parts of its neighbours. The Figure 3.4. shows the model result of mean temperature for 1990-2000 and the Figure 3.5. belongs to mean precipitation for the same decade.

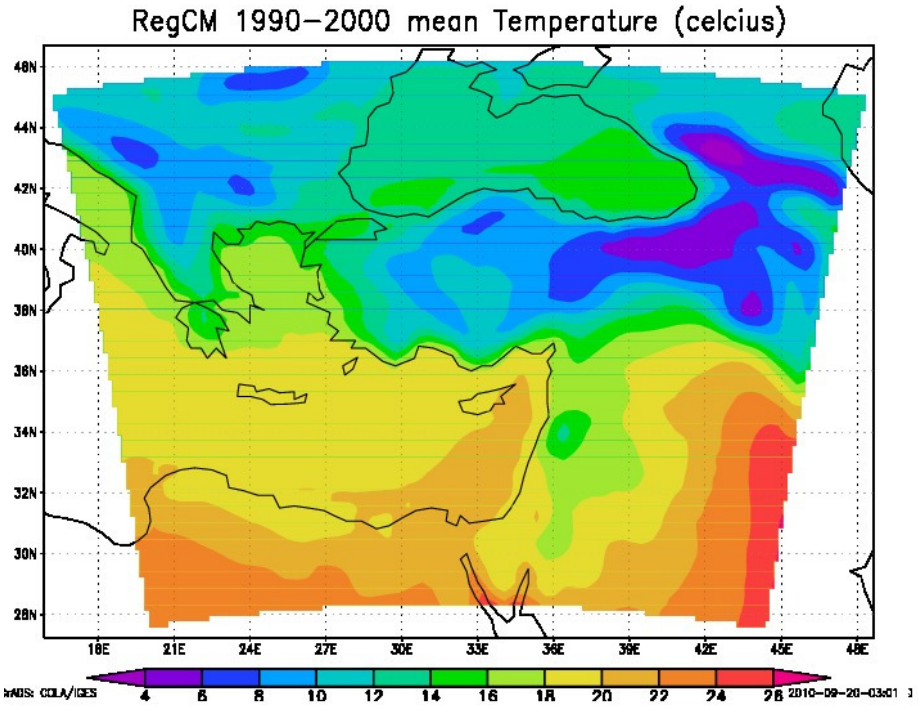

Figure 3.4. Mean temperature in Celsius for 1990-2000.

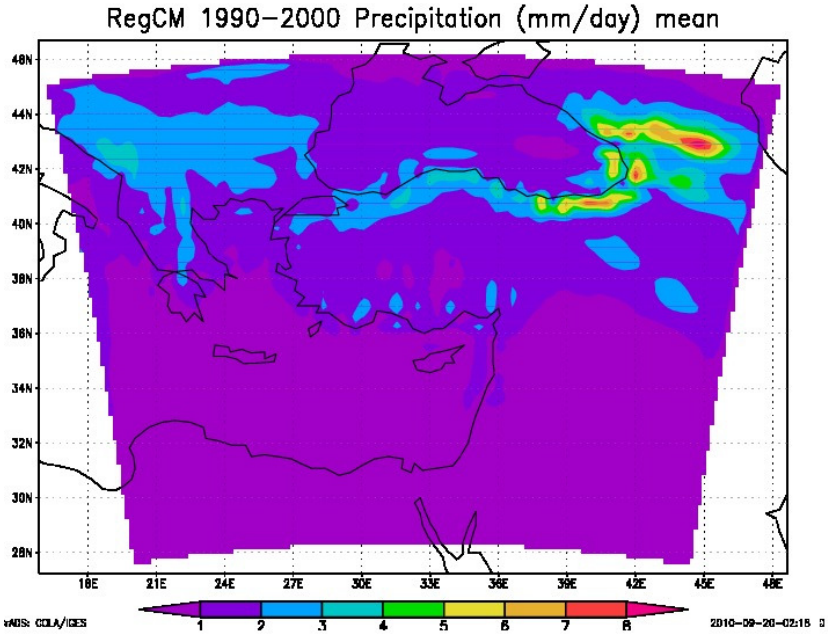

Figure 3.5. Mean precipitation in mm per day for 1990-2000.

To see the validation of the model output, the results were compared with the observation data. The Climatic Research Unit (CRU) of East Anglia University gridded datasets, which have been developed from data acquired from weather stations around the world, were used for comparison. The difference between the model result and the gridded data was well-matched. For example, Figure 3.6. shows the difference for temperature between the CRU and RegCM-4.0.

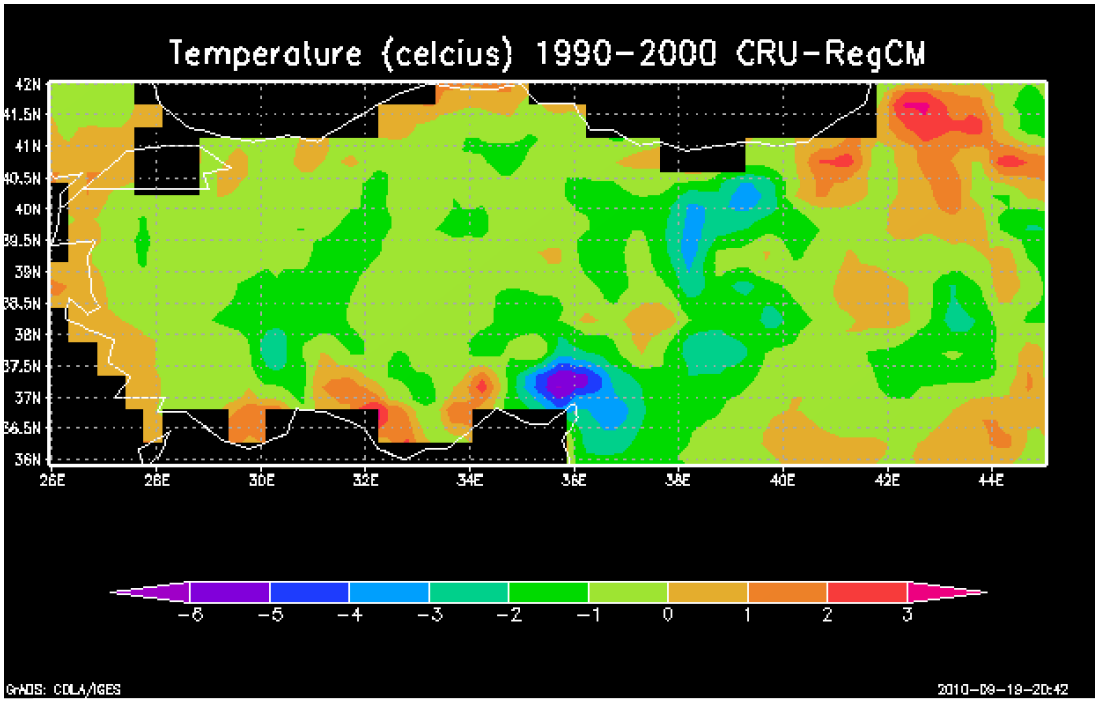

Figure 3.6. CRU – RegCM comparison for temperature between 1990 and 2000.

After this considerable result, the NAOI were calculated for 2040-2050 and 2090-2100. For prediction of future NAOI, the regression analysis was enforced and the CRU datasets were used for 1990-2000 instead of using RegCM-4.0 to minimize of station data errors. However, the RegCM-4.0 outputs were used for the data of future. The precipitation variables were ignored because of its correlation coefficient with the NAOI approximately zero (Figure 3.7.)

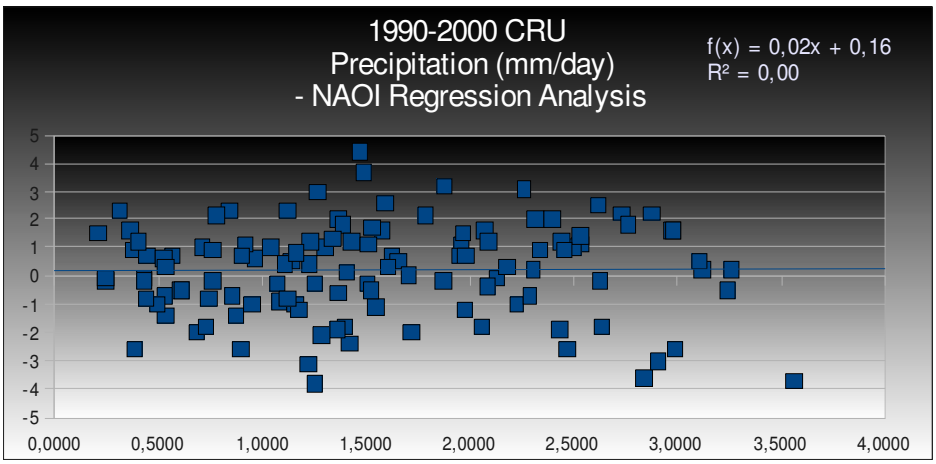

Figure 3.7. Statistical relationship between the CRU monthly total precipitation data and the NAOI.

Before the NAOI predictions for 2040-2050 and 2090-2100 had been done, observation data of the NAOI and the predicted NAOI were compared with each other for the period of 1990-2000. The NAOI predictions for decade were computed based on gridded temperature data (the CRU temperature data).

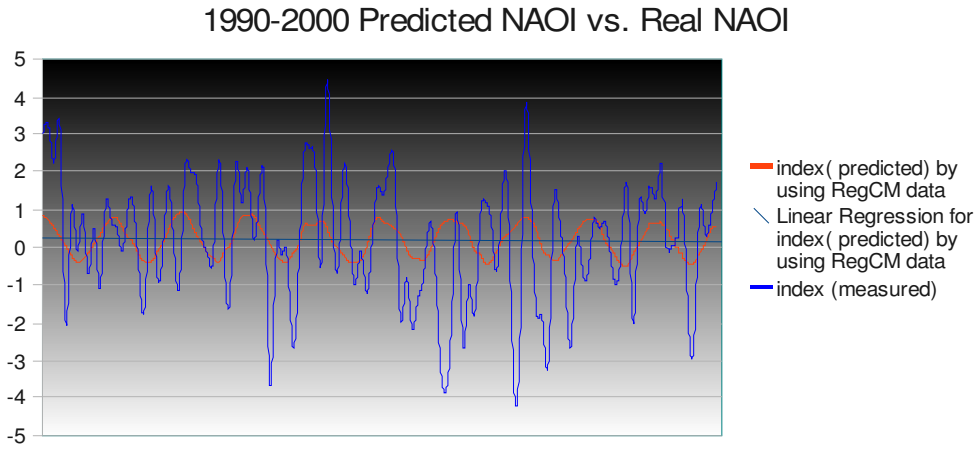

Figure 3.8. Comparison of the station based NAOI and the predicted NAOI. In this graphic, the red line refers to the index that is predicted by using regression coefficients obtained by the regression analysis of 1990 – 2000 CRU data and the NAOI; and the blue line refers to the real NAOI that is measured.

As is seen in the Figure 3.8., while the station based NAO indices were varying between -4.5 and +4.5, the predicted values were varying between -1 and +1 by drawing an oscillation.

Although it was not a good result, the predictions of the NAOI were computed for terms of 2040-2050 and 2009-2100 via the Equation 3.1. that is derived from the relationship between the CRU temperature and the NAOI for 1990-2000.

$$Y = -0{,}0542\ X + 0{,}86 \qquad (3.1.)$$

To be able to obtain the future NAOI, the regression coefficients that were obtained from the Equation 3.1., were used. Figure 3.9. shows the graphic of the predicted NAOI for 2040-2050 and Figure 3.10. shows the graphic of the predicted NAOI for 2090-2100.

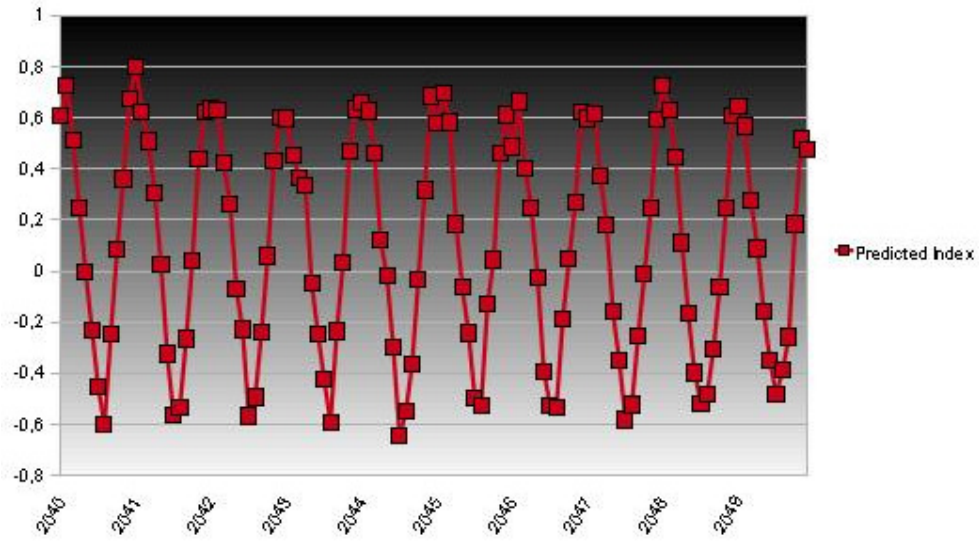

Figure 3.9. The predicted values of the NAOI for 2040-2050.

In each cases, the future indices of the North Atlantic Oscillation were varied between -1 and +1.

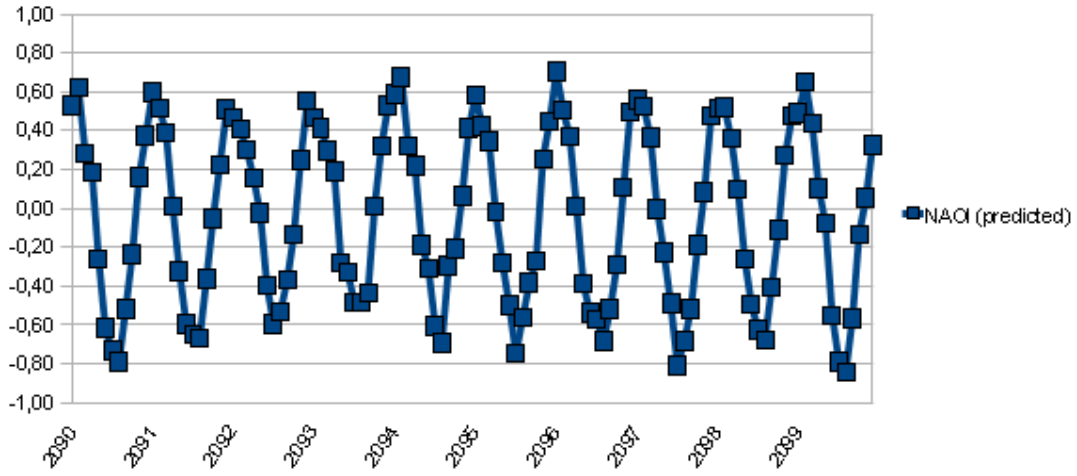

Figure 3.10. The predicted values of the NAOI for 2090-2100.

The same prediction values were calculated for the station of Amasra. Even though Amasra station has a higher correlation coefficient, it showed the similar results during the prediction of the NAOI. The predicted values were generally varied between -1 and +1, except 2041-January (+1,02) and 2099-August (-1,01). Figure 3.11 and Figure 3.12 show the variations of predicted North Atlantic Oscillation indices for Amasra station.

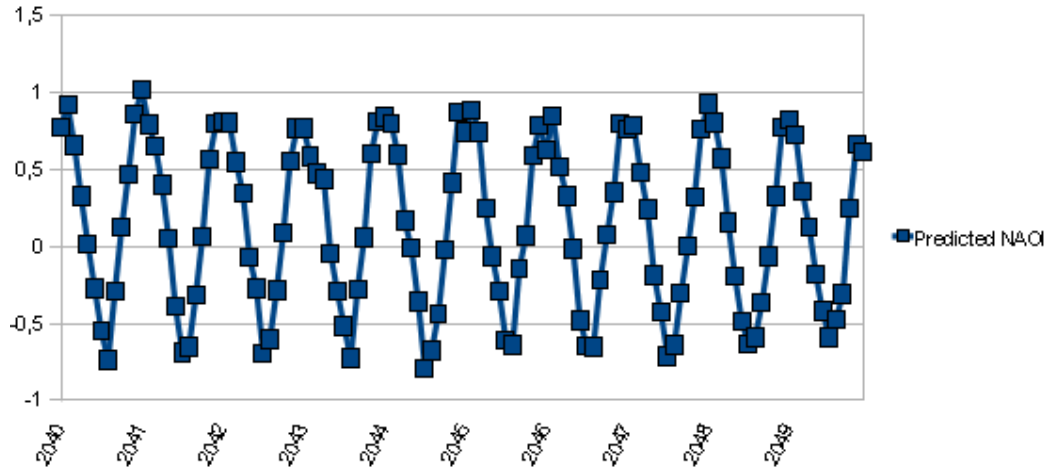

Figure 3.11. The predicted values of the NAOI for Amasra (2040-2050).

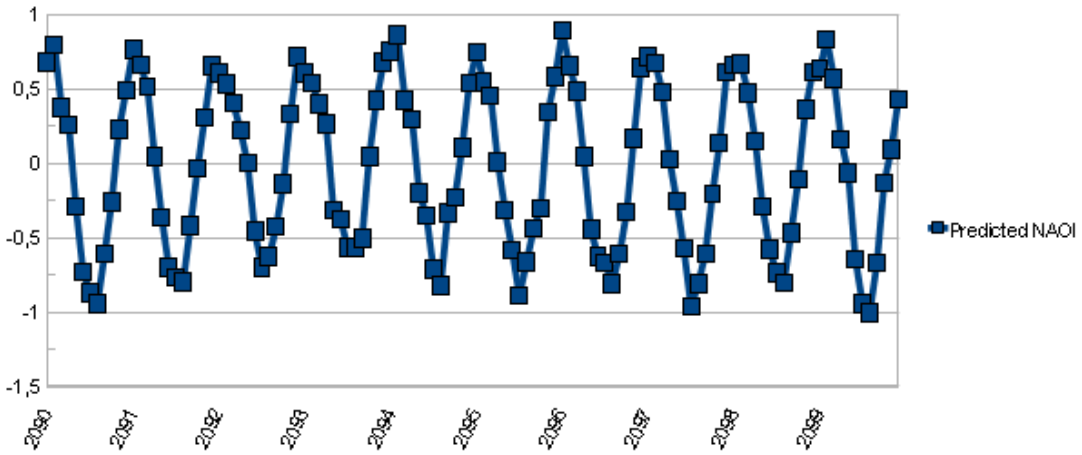

Figure 3.12. The predicted values of the NAOI for Amasra (2090-2100).

4. CONCLUSIONS, DISCUSSIONS AND RECOMMENDATIONS FOR FUTURE STUDIES

The North Atlantic Oscillation (NAO) is an important mode of variability in the Northern Hemisphere influencing the climate fluctuations from the eastern seaboard of the United States to Siberia and from the Arctic to the subtropical Atlantic. Although observational and modeling evidence proves that forecasting of the NAO is theoretically possible, a major difficulty in outlining a comprehensive strategy for the NAO prediction is the extreme complexity of the phenomenon as it involves different mechanisms with different characteristic time scales from several days to decades. The management of energy resources and agricultural yields can benefit from the prior knowledge of the NAO phases in Turkey as well as in almost all the countries affected. An economic benefit associated with the use of the NAO prediction can be assessed for potential users as the ratio between the costs of their action to prevent NAO related damages, and the loss that they incur in case they do not protect their operations.

The results of this study show us that there is statistically an inverse relationship between the temperature and precipitation of Turkey, and the North Atlantic Oscillation. Even though the results are in agreement with previous studies about the correlation's direction, the coefficients of the correlations are not enough strong to make future index predictions.

We know that the NAO is so dominant during the winters. The highest correlation coefficients (nearly 0.70) can be seen in this season. This study proved that annual analyses of the NAO may not be clear. However, the other factor which decreases the correlation can be the data type. Studying with the station datasets implies more errors or noises. To study by using the other data type for indices and the climatic variables could give us better results. At this time, using station data of temperature and precipitation for Turkey have got some problems because of the properties of local physical geography.

In conclusion, the effects of the North Atlantic Oscillation can be seen obviously with the better parameterization and choices. Instead of studying annual or studying with local station data, one can study seasonal with grid data and the other types of indices. Another solution may be studying regional and to choose a specific area with a homogeneous distribution of stations. Ultimately, comparison of the other parameters such as pressure, maximum and minimum temperatures, wind velocities rather than merely precipitation and air temperature can help us to make better predictions. Clearly, more work needs to be done in order to better understand the driving forces behind the NAO. This would potentially allow better prediction of the NAO, which could lead to better monthly and seasonal temperature or precipitation predictions.

REFERENCES

1. National Weather Service, Climate Prediction Center, http://www.cpc.noaa.gov/, 2010.

2. Hurrell et al., in The North Atlantic Oscillation: Climate Significance and Environmental Impact, Geophysical Monograph 134, American Geophysical Union, 2003.

3. Barnston, Anthony G. and Robert E. Livezey, Classification, Seasonality and Persistence of Low-Frequency Atmospheric Circulation Patterns, Monthly Weather Review, Volume 115, pp. 1083-1126, 1986.

4. Wallace, John M. and David S. Gutzler, Teleconnection in the Geopotential Height Field during the Northern Hemisphere Winter, Monthly Weather Review, Volume 109, pp. 784-812, 1980.

5. Van Loon, Harry and Jeffery C. Rogers, The Seesaw in Winter Temperature between Greenland and Northern Europe. Part 1: General Description, Monthly Weather Review, Volume 106, pp.296-310, 1977.

6. Van Loon, Harry and Jeffery C. Rogers, The Seesaw in Winter Temperature between Greenland and Northern Europe. Part 2: Some Oceanic and Atmospheric Effects in Middle and High Latitudes, Monthly Weather Review, Volume 107, pp.509-519, 1979.

7. Trigo, Ricardo M., Timothy J. Osborn and Joao M. Corte-Real, The North Atlantic Oscillation influence on Europe: climate impacts and associated physical mechanisms, Climate Research, Vol.20: 9-27, pp. 9-17, 2002.

8. Hurrell, Jim, NCAR CGD's climate Analysis Section, http://www.cgd.ucar.edu/cas/jhurrell/, 2010.

9. Hurrell, J. W. and C. Deser, North Atlantic climate variability: The role of the North Atlantic Oscillation. *J. Mar. Syst.*, **78**, No. 1, pp. 28-41, DOI:10.1016/j.jmarsys.2008.11.026, 2009.

10. Jones, P.D., T. Jonsson and D. Wheeler, Extension to the North Atlantic Oscillation using early instrumental pressure observations from Gibraltar and South- West Iceland. Int. J. Climatol. 17, pp. 1433-1450, 1997.

11. Rogers, J.C., North Atlantic storm track variability and its association to the North Atlantic Oscillation and climate variability of Northern Europe. Journal of Climate 10(7), pp.1635-1647, 1997.

12. Hurrell, J.W., Decadal trends in the North Atlantic Oscillation and relationships to regional temperature and precipitation. Science 269, pp. 676-679, 1995.

13. Windows to Universe, http://www.windows2universe.org/earth/climate/nao.html, 2010.

14. UCAR – University Corporation for Atmospheric Research, http://www2.ucar.edu/, 2010.

15. SECAM, University of Exeter, North Atlantic Oscillation, http://www1.secam.ex.ac.uk/cat/NAO, 2010.

16. North Atlantic Oscillation, http://www.ldeo.columbia.edu/res/pi/NAO/, 2010.

17. Serreze, Mark C., Fiona Carse and Roger G. Barry, Icelandic Low Cyclone Activity: Climatological Features, Linkages with the NAO, and Relationship with Recent Changes in the Northern Hemisphere Circulation, Journal of Climate, Volume 10, pp. 453-464, 1997.

18. Hurrell, James W., Decadel Trends in the North Atlantic Oscillation: Regional Temperatures and Precipitation, Science, New Series, Vol. 269, No. 5524, pp. 676-679, 1995.

19. Ben-Gai, T. et al., Temperature and Surface Pressure Anomalies in Israel and the North Atlantic Oscillation, Theoretical and Applied Climatology, Vol.69, pp.171-177, 2001.

20. Werner, A. and C. D. Schönwiese, A Statistical Analysis of the North Atlantic Oscillation and Its Impact on European Temperature, The Global Atmosphere and Ocean System, Vol. 8, No. 4, pp. 293–306, 2002.

21. Xoplaki, E., Climate Variability over the Mediterranean, PhD dissertation, University of Bern, Switzerland, 2002.

22. Hasanean, H. M., Wintertime Surface Temperature In Egypt In Relation to the Associated Atmospheric Circulation, International Journal of Climatology, Vol. 24, pp. 985-999, 2004.

23. Türkeş, Murat and Ecmet Erlat, Precipitation Changes and Variability in Turkey Linked to the North Atlantic Oscillation During the Period 1930-2000, International Journal of Climatology, Vol. 23, pp.1771-1796, 2003.

24. Türkeş, Murat and Ecmet Erlat, Climatological Responses of Winter Precipitation in Turkey to variability of the North Atlantic Oscillation During the Period 1930-2001, Theoretical and Applied Climatology, Vol. 81, pp. 45-69, 2005.

25. Türkeş, Murat and Ecmet Erlat, Winter Mean Temperature Variability in Turkey Associated with the North Atlantic Oscillation, Meteorol Atmos Phys, Vol. 105, pp. 211-225, 2009.

26. Feidas, H. et al., Trend Analysis of Air Temperature Time Series in Greece and Their Relationship with Circulation Using Surface and Satellite Data: 1955-2001, Theoretical and Applied Climatology, Vol. 79, pp. 185-208, 2004.

27. Von Storch, Hans and Francis W. Zwiers, Statistical Analysis in Climate Research, Cambridge University Press, 2004.

28. Wilks, Daniel S., Statistical Methods in the Atmospheric Sciences, Second Edition, 1995.

29. Regression Analysis, http://en.wikipedia.org/wiki/Regression_analysis, 2010.

30. Cook, R. Dennis and Sanford Weisberg, Criticism and Influence Analysis in Regression, Sociological Methodology, Vol. 13, pp. 313,361, 1982.

31. Houghton, John, Global Warming, The Complete Briefing, Third Edition, Cambridge University Pres, 2004.

32. The First Climate Model, http://celebrating200years.noaa.gov/breakthroughs/climate_model/welcome.html, 2010.

33. Modelling the Climate, http://climateprediction.net/content/modelling-climate, 2010.

34. Regional Climate Models, http://climateprediction.net/content/regional-climate-models, 2010.

35. Giorgi et al., RegCM Version 4.0 User's Guide, pp. 1-24, Trieste, Italy, 2010.

36. Coppola, Erica, Regional Climate Modeling Lecture 1, 2009.